Received: 21 October 2022 | Revised: 25 June 2023 | Accepted: 26 June 2023

DOI: 10.1002/hyp.14937

RESEARCH ARTICLE

WILEY

Rainfall-runoff responses and hillslope moisture thresholds for an upland tropical catchment in Eastern Madagascar subject to long-term slash-and-burn practices

B. W. Zwartendijk[1,2] | H. J. van Meerveld[3] | A. J. Teuling[1] | C. P. Ghimire[4] | L. A. Bruijnzeel[5,6]

[1]Hydrology and Quantitative Water Management Group, Wageningen University & Research, Wageningen, The Netherlands

[2]Inholland University of Applied Sciences, Alkmaar, The Netherlands

[3]Department of Geography, University of Zurich, Zurich, Switzerland

[4]AgResearch, Lincoln Research Centre, Christchurch, New Zealand

[5]Department of Geography, King's College London, London, UK

[6]Institute of International Rivers and Eco-Security, Yunnan University, Kunming, People's Republic of China

Correspondence
B. W. Zwartendijk, Inholland University of Applied Sciences, Bergerweg 200, 6700 HB Alkmaar, The Netherlands.
Email: bob.zwartendijk@inholland.nl

Funding information
ESPA; Nederlandse Organisatie voor Wetenschappelijk Onderzoek; ESPA programme of the UK, Grant/Award Number: 050/14/MEF/SG/DGF/DCB.SAP/SCB; Dutch Research Council (NWO), Grant/Award Number: 023.016.033

Abstract

Slash-and-burn agriculture is an important driver of tropical forest loss and typically results in a mosaic of land uses. However, there is little quantitative information about the hydrological effects of long-term slash-and-burn agriculture and how such mosaics affect the rainfall-runoff response at the catchment scale. We monitored streamflow responses at two points along a perennial stream in a 31.7 ha catchment in eastern Madagascar that was monitored previously between 1963 and 1972. Land cover in 2015 consisted of degraded grasslands, shrub and tree fallows at various stages of regrowth (64%), eucalypt stands for charcoal production (30%), and rice paddies and wetlands in the valley-bottom (3%). For the majority (60%) of the events during the study period, the ratio between the total amount of stormflow and rainfall was <3%, suggesting that for these events runoff was generated in the valley-bottom only. Events for which an antecedent soil moisture storage plus rainfall (ASI + *P*) threshold was exceeded had much higher stormflow ratios (up to 50%), indicating that a certain wetness was required for the hillslopes to contribute to stormflow. Stable isotope sampling for four small to moderate events indicated that stormflow was dominated by pre-event water. Total stormflow and annual water yield in 2015 were higher than in the 1960s, despite much lower rainfall in 2015. We attribute these differences to changes in soil physical properties caused by the repeated burning and loss of top-soil, which has resulted in a reduction in the depth to the impeding layer. The changed runoff-processes (less infiltration, more saturation-excess overland flow) thus affect local water resources.

KEYWORDS
runoff generation processes, saturation-excess overland flow, stable isotopes, stormflow, swidden agriculture, threshold response

1 | INTRODUCTION

Slash-and-burn agriculture, also known as swidden agriculture or shifting cultivation, is the dominant driver of forest loss in large parts of Africa and South-East-Asia, and, to a lesser extent Latin America (Curtis et al., 2018; Feng et al., 2021; Heinimann et al., 2017). The practice typically produces a mosaic of land uses, including cultivated fields, vegetation at various stages of regrowth, and in extreme cases, fire-

maintained grasslands (Chazdon, 2014; Mukul & Herbohn, 2016; Van Vliet et al., 2012). Repeated burning generally leads to decreases in soil faunal biomass and activity, organic carbon content, and root density (Fragoso et al., 1997; Huon et al., 2013; Lavelle et al., 2001; Ziegler et al., 2009), with corresponding reductions in soil infiltration capacity and the near-surface saturated soil hydraulic conductivity (K_{sat}; Patin et al., 2012; Shougrakpam et al., 2010; Zhang et al., 2019; Ziegler et al., 2004; Zwartendijk et al., 2017). This can lead, in turn, to an increase in the frequency and magnitude of overland flow (Bonell et al., 2010; Lacombe et al., 2018; Podwojewski et al., 2008; Toky & Ramakrishnan, 1981; Zwartendijk, Ghimire, et al, 2020, Zwartendijk, van Meerveld et al., 2020), with ensuing increases in surface erosion and loss of soil fertility (Malmer et al., 2005; Patin et al., 2018; Sandevoir et al., 2023; Ziegler et al., 2009), and increased risk of downstream flooding and sedimentation (Brookhuis & Hein, 2016; Valentin et al., 2008). However, top-soil infiltration rates normally improve again during vegetation regrowth, resulting in less overland flow and a diminished or more delayed runoff response to rainfall (Chandler & Walter, 1998; Fritsch, 1993; Lozano-Baez et al., 2018; van Meerveld et al., 2019). Thus, in catchments with slash-and-burn agriculture, where the landscape is characterised by a mosaic of degrading cropped fields and regenerating fallows, hydrological processes can be expected to vary accordingly, both spatially and temporally (Bailly et al., 1974; Gafur et al., 2003; Ribolzi et al., 2018; Sandevoir et al., 2023; Toky & Ramakrishnan, 1981; Ziegler et al., 2004).

Plot-scale runoff responses for the different land uses depend on the K_{sat} profile of the soil (Chappell et al., 2007; Elsenbeer et al., 1999; Zwartendijk, Ghimire 2020, Zwartendijk, van Meerveld et al., 2020), which depends, in turn, on the past land use. Previous land use affects the K_{sat} profile directly in terms of the degree of previous soil degradation and compaction, and indirectly through the loss of top-soil via erosion (Chandler & Walter, 1998; Lozano-Baez et al., 2018; Patin et al., 2012; Zhang et al., 2019; Ziegler et al., 2004). The shallower the depth to an impeding layer, the lower the storage capacity of the soil and the greater the likelihood that hillside saturation-excess overland flow (SOF) becomes an important runoff mechanism during times of high rainfall (Birch et al., 2021b; Bonell, 2005; Elsenbeer et al., 1992; Zwartendijk, Ghimire, et al., 2020, Zwartendijk, van Meerveld et al., 2020).

However, the runoff response at the catchment scale cannot simply be deduced from the sum of the responses of individual vegetation patches or hillslopes (Uchida et al., 2005; Uchida & Asano, 2010). It also depends on hillslope topography and morphology (Janeau et al., 2003; Lapides et al., 2020; Ribolzi et al., 2011), the presence of roads and footpaths (Rijsdijk et al., 2007; Sandevoir et al., 2023; Ziegler et al., 2004), and the hydrological connectivity between the different patches or hillslopes and the stream (Asano & Uchida, 2018; Ribolzi et al., 2018; Robinson et al., 1995). The degree of connectivity also depends on rainfall characteristics and antecedent wetness conditions (Ries et al., 2017; Tobón & Bruijnzeel, 2021; Western et al., 1999; Xu et al., 2019). Numerous studies have reported the existence of a wetness threshold for catchment-scale runoff responses, which is conventionally interpreted to reflect the increase in hillslope-stream connectivity as the catchment wets up (e.g., Birch et al., 2021b; Gomi et al., 2008; Litt et al., 2015; Tobón & Bruijnzeel, 2021; Zhang, van Meerveld, et al., 2018).

Although changes in K_{sat}, dominant flow paths, and runoff responses after converting tropical forest to pasture, agricultural cropping, or extractive plantations are well-documented (Birch et al., 2021a, 2021b; De Moraes et al., 2006; de Vries et al., 2022; Liu et al., 2011; Nespoulous et al., 2019; Recha et al., 2012; Scheffler et al., 2011; Toohey et al., 2018; Zimmermann et al., 2006), integrated work in tropical catchments that have experienced *multiple* cycles of slash and burn agriculture is rare (Bailly et al., 1974; Ribolzi et al., 2018; Sandevoir et al., 2023; van Meerveld et al., 2019; Zhang, van Meerveld, et al., 2018). Therefore, we examined the effects of soil- and hillslope characteristics on catchment-scale stormflow generation in an upland catchment in eastern Madagascar that had been investigated in the 1960s by French researchers (Bailly et al., 1974) and has experienced slash-and-burn agriculture ever since. In addition, parts of the catchment are in use for charcoal production by repeated coppicing and burning of *Eucalyptus* trees. Our previous work in the area has revealed important differences in near-surface K_{sat} between the different land covers (Zwartendijk et al., 2017), which result in distinctly different perched water table and overland flow responses (van Meerveld et al., 2021; Zwartendijk, Ghimire et al., 2020, Zwartendijk, van Meerveld et al., 2020). In this follow-on study, we examine the runoff response at the catchment scale and address the following research questions:

- What are the dominant sources of streamflow during rainfall events of different magnitude and intensity?
- Is there a wetness threshold above which stormflow increases markedly, and above which hillslopes are more likely to contribute to stormflow?
- Has the rainfall-runoff response intensified since the 1960s as a result of long-term slash-and-burn activity and associated soil degradation?

2 | STUDY SITE DESCRIPTION

The 31.7 ha Marolaona catchment is located near Andasibe in the Ankeniheny Zahamena corridor in eastern Madagascar (18.970°S, 48.422°E; Figure 1). It is drained by a 920-m long perennial stream. Land use in the catchment and the region is dominated by small-scale subsistence farming based on slash-and-burn practices (Styger et al., 2007). Typically, rain-fed rice is grown for one or two seasons, sometimes followed by root crops like cassava for one or two more seasons before the fields are abandoned until the next slash-and-burn cycle begins. Due to increased population pressure and limited available land, the time between successive cycles in the area has decreased from the traditional 8–15 years to 3–5 years (Styger et al., 2007).

The catchment's land use in the 1960s included agricultural fields, and a mixture of shrub- and tree fallows (Bailly et al., 1974). Land use was still very patchy during the 2015–2016 follow-up study (Figure 1) and consisted mainly of tree fallows (< 15 years old, 43%), irregularly coppiced and burned eucalypt plantations for charcoal production with an understorey dominated by *Imperata cylindrica* and *Aristida*

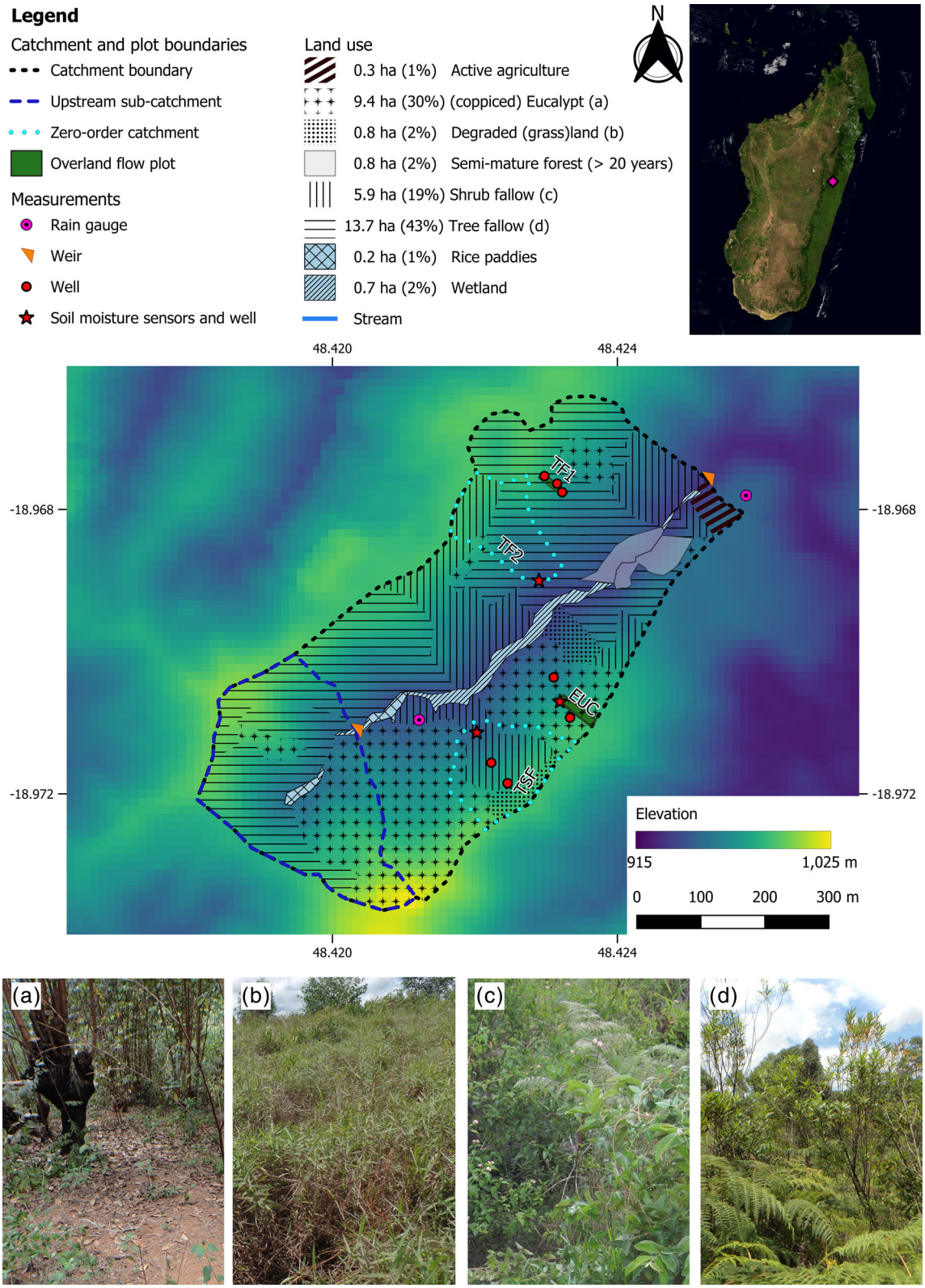

FIGURE 1 Map of the Marolaona catchment showing the land use in 2015, and the locations of the rainfall gauges, stream gauges (i.e., weirs), soil moisture sensors, shallow groundwater wells, and overland flow plots. Inset: catchment location in Madagascar. Imagery: True Marble 500 m (Unearthed Outdoors, 2007 http://www.unearthedoutdoors.net/global_data/true_marble/download, downloaded on 2 October 2015). Photos of the main land covers in the catchment: coppiced *Eucalyptus* (a), degraded grassland (b), shrub fallow (c), and tree fallow (d).

similis grasses (30%), and shrub fallows (<5 years old, 19%). The remaining 8% of the catchment was covered by small patches of fire-related grassland (2%), semi-mature forest (>20 years old, 2%), agricultural fields (rain-fed, 1%), and irrigated rice cultivation (1%) and wetlands (2%) in the flat valley bottom (Figure 1). The stream, the rice paddies and the wetlands occupied ~3% of the total catchment area (and 25%, 17% and 58% of the valley-bottom area, respectively). The dominant tree species in the tree fallows were native *Psiadia altissima* and *Harungana madagascariensis*, plus the native shrub *Clidemia hirta*, the fern *Pteridium aquilinum* and the invasive shrubs *Lantana camara* and *Rubus moluccanus* (Zwartendijk, Ghimire et al., 2020, Zwartendijk, van Meerveld et al., 2020; *cf*. Styger et al., 2007).

Mean annual rainfall at the Andasibe weather station (990 m a.s.l.; ~5 km from the study catchment) between 1983 and 2013 was 1625 mm (range: 1124–2068 mm). Monthly rainfall totals between December and March exceed 200 mm on average, and are <100 mm between April and October (Météo Madagascar, unpublished data). The wettest month during the study period was February 2015, with 403 mm of rain. The average temperature was 15°C during the dry season (April–October 2015) and 22°C during the wet season (November 2014–March 2015; Ghimire et al., 2022).

The elevation in the catchment ranges from 930 to 1025 m a.s.l. (Figures 1 and S1). Slopes are moderate to steep (10–50°, average 21°), relatively short (60–300 m), and generally convexo-concave. Depth to the underlying Precambrian metamorphic and igneous bedrock exceeds 6 m (Zwartendijk, Ghimire et al., 2020, Zwartendijk, van Meerveld et al., 2020). The soils (Tropudults) have a sandy clay loam to clayey texture (up to 45% clay at the surface, increasing slightly with depth; Andriamananjara et al., 2016). K_{sat} decreases rapidly with depth (catchment-wide median values of ~500 mm h^{-1} at the surface, ~20 mm h^{-1} at 10–20 cm, and ~2 mm h^{-1} at 20–30 cm; Zwartendijk, Ghimire, et al., 2020) and differs between land-cover types. The highest surface K_{sat} values are associated with eucalypt stands and tree fallows (median values of ~960 and ~460 mm h^{-1}, respectively) and the lowest with degraded grasslands (median of 42 mm h^{-1}; Zwartendijk, Ghimire, et al., 2020).

3 | METHODS

3.1 | Field and laboratory measurements

3.1.1 | Rainfall

Rainfall was measured between 3 February 2015 and 3 March 2016 using two tipping-bucket rain gauges (Rain Collector II, Davis Instruments, Hayward, USA; 0.2 mm per tip) connected to HOBO Pendant event loggers (Onset Computer Corporation, Bourne, USA). The gauges were installed at ~1.2 m above the soil surface to avoid ground-splash effects (see Figure 1 for locations). Differences in recorded rainfall amounts for the two gauges were very small (0.8% difference for total amount; *cf*. Zwartendijk, van Meerveld, et al., 2020). Since the record for the rain gauge near the catchment outlet was complete, only those data were used in this study.

3.1.2 | Streamflow

Suppressed (rectangular) broad-crested weirs were constructed in the early 1960s to measure streamflow at the catchment outlet and for an upstream sub-catchment (7.1 ha) (Bailly et al., 1974; see Figure 1 for locations). We repaired the weirs and replaced the upper weir by a 90° sharp-crested V-notch. Stream water levels were measured at 5-min intervals. Due to sensor failure, water level data are only available for two periods: (i) 15 February–13 May 2015 (88 days); and (ii) 12 December 2015–2 March 2016 (82 days).

During the first period, water levels were measured with a CTD-10 sensor (Decagon Devices, Pullman, USA) connected to an EM50-logger (Decagon Devices). During the second period, water levels were measured with an STS DL/N 70 pressure transducer (Sensor Technik, Sirnach AG, Switzerland). Streamflow at the lower weir was measured using the salt-dilution-slug-injection method (Moore, 2004; Moore, 2005) over a range of flow conditions to establish the rating curve (Supporting Information section 2.1). The rating curve for the upper weir was based on the equations for a truncated triangular sharp-crested weir (Bos, 1989; Jan et al., 2006), validated by volumetric measurements (Supporting Information section 2.2).

3.1.3 | Soil moisture and groundwater levels

Volumetric soil moisture contents were measured at 5, 15 and 30 cm depth in three hillslope plots: TF2 (young tree fallow, 1.58 ha), EUC (irregularly coppiced *Eucalyptus robusta* trees with degraded fire-related grassland, 0.05 ha) and TSF (terraced shrub fallow, 1.93 ha) (Zwartendijk, van Meerveld, et al., 2020). The three depths for the soil moisture sensors were based on the rapid decline in K_{sat} with depth below the surface (Zwartendijk, Ghimire, et al., 2020). Perched water tables (PWT) were measured in three fully screened wells in the TF1 (young tree fallow, 0.05 ha), EUC and TSF plots, and one well in the TF2 plot (see Figure 1 for locations). Further details are provided by Zwartendijk, van Meerveld, et al. (2020). The PWT time-series for plots TF2 (lower slope position) and EUC (mid-slope) were used for statistical comparisons with the discharge time-series.

3.1.4 | Water sampling for stable isotope analysis

Samples of streamflow and overland flow (lined gutters of plots TF2, EUC and TSF) were taken before, during and after rainfall events. A rainfall sample was taken for every 13 mm of rain using a sequential sampler (Kennedy et al., 1979) installed next to the recording rain gauge near the catchment outlet (Figure 1). The sampler was emptied before 10 AM on the day after an event. In January and February 2016 (wet season) daily bulk rainfall samples were taken from the rain gauge at plot TF2 (emptied daily around 8 AM). In total, we collected 39 rainfall samples (26 from the sequential rainfall sampler and 13 bulk samples), 209 streamflow samples (173 at the lower weir and 36 at the upper weir), and 31 overland flow samples (6 at TF1, 10 at TF2, 8 at TSF and 7 at EUC).

All water samples were analysed for the stable isotopes of oxygen and hydrogen using a Cavity Ring-Down Spectroscope (L2130-i (CRDS), Picarro Inc., Santa Clara, USA) at the laboratory of the Chairs of Hydrology at the University of Freiburg (Germany). The isotope ratios were expressed relative to the Vienna Standard Mean Ocean Water using the delta notation. The stated precision was ±0.16‰ for $\delta^{18}O$ and ±0.6‰ for $\delta^{2}H$. All samples plotted on or near the local meteoric waterline, suggesting that the samples were not affected by isotopic fractionation (Figure S7).

3.2 | Analyses of field data

3.2.1 | Event definition

To determine streamflow response characteristics, rainfall events were defined as periods with more than 5 mm of rainfall, followed by a dry period of at least three hours (*cf*. Ghimire et al., 2014; Zwartendijk, van Meerveld, et al., 2020). For inclusion in the analysis, streamflow responses at either weir had to exceed an arbitrary threshold value of 0.02 mm h^{-1}.

There were 25 rainfall events during the first period (15 February–13 May 2015; total rainfall: 537 mm). For two events, stream responses at the catchment outlet did not meet the criterion for minimum flow increase. Also, there were no reliable stormflow data for the upper weir for ten events during the first period due to blockage of the air vent. Hence, complete streamflow data during this period were available for 23 events at the catchment outlet and only 15 events at the upper weir. During Period 2 (12 December 2015–2 March 2016; total rainfall: 473 mm), there were also 25 rainfall events but no clear streamflow responses were observed for 20 (lower weir) and (upper weir) events. Thus, complete streamflow responses during the second period were available for only five events at the outlet and for 19 events at the upper weir. The combined data from the two periods (50 rainfall events, 28 streamflow responses at the outlet and 34 at the upper weir) were used in the analyses.

3.2.2 | Rainfall characteristics and antecedent wetness conditions

For each rainfall event we computed the rainfall amount (*P*), duration, average intensity, the maximum and median hourly and 5-min rainfall intensities, and the time of the centroid of the event. As measures of antecedent wetness conditions, we calculated the total rainfall during the three (AP_3) and seven days (AP_7) prior to each event, stream discharge at the start of the event (Q_0), and an *antecedent soil moisture index* (ASI) for the top 30 cm of the soil at the *Eucalyptus* plot (ASI_{EUC}) and the tree fallow plot (ASI_{TF2}). The ASI represents the total storage in the upper 30 cm of the soil and is calculated as the sum product of the volumetric moisture contents at the 0–10 cm, 10–22.5 cm and 22.5–30 cm depth intervals; (*cf*. Zwartendijk, van Meerveld, et al., 2020).

3.2.3 | Streamflow response characteristics

For each rainfall event that produced a streamflow response, the end of the response was determined using the 'constant-*k* method' (Blume et al., 2007). The total stormflow amount (Q_s) was computed by subtracting a constant baseflow rate (Q_0) from the streamflow during the response. The *stormflow ratio* is the ratio between the total stormflow amount and event rainfall (Q_s/P). The stormflow ratio is equivalent to the so-called Minimum Contributing Area (MCA), that is, the fraction of the catchment that would yield the measured stormflow if it contributed 100% of the rainfall it received (Dickinson & Whiteley, 1970). The total stormflow and stormflow ratio were calculated for individual events and for the two observations periods. We similarly calculated the total streamflow amount (*Q*) and the *runoff ratio* (*Q*/*P*) for the considered individual events and the entire observation period.

We, furthermore, determined for each event the maximum flow rate (*peak-flow*; Q_p), and the following timing-related response characteristics: *response lag time* (time between the start of rainfall and the first increase in stream water level), *lag to peak* (time between start of rainfall and peak flow), *stormflow duration* (the time between the start and end of stormflow) and *centroid lag time* (the time between the centroids of rainfall and streamflow).

3.2.4 | Hydrograph separation

Only four of the sampled rainfall events had a sufficient number of stream water samples, a noticeable streamflow response, and contrasting $\delta^{18}O$ values for rainfall and baseflow. For these events we applied a two-component hydrograph separation to determine the *event-water* (Q_e) and *pre-event water* (Q_{pe}) contributions to streamflow (Klaus & McDonnell, 2013; Sklash & Farvolden, 1979). The $\delta^{18}O$ value of the baseflow prior to the event was used to represent the pre-event stream water composition. For events for which only a single bulk rainfall sample was available, the isotopic composition of this sample was taken as the event-water composition. For events for which multiple rainwater samples were available, the event-water composition was based on the incremental weighted mean (McDonnell et al., 1990). The uncertainty in the event-water contribution to streamflow was calculated following the method of Genereux (1998).

We used linear interpolation of the event-water contribution (i.e., the percentage of event water in streamflow) between the individual isotope sampling times to obtain a continuous time series of event water and pre-event water (van Meerveld et al., 2019; von Freyberg et al., 2018) and to determine the average event-water contribution (i.e., the average percentage of event water in streamflow; Q_e/Q). We furthermore, determined the percentage of rainfall that became

TABLE 1 Rainfall and streamflow totals at the lower weir (entire catchment of 31.7 ha) for different periods.

	Period 1: 15 Feb–13 May 2015	Simulated: 14 May 2015–11 Dec 2015	Period 2: 12 Dec 2015–3 Mar 2016	Year: 15 Feb2015–14 Feb 2016	Year: 1 Mar 2015–29 Feb 2016
Rainfall (mm)	537	398	466	1314	1103
Total streamflow (Q) (mm)	372	174[†]	116	640[b]	574[b]
Runoff ratio (Q/P) (%)	69	44[a]	25	48[b]	52[b]
Stormflow (Q_s) (mm)	4	2[a]	16	57[b]	34[b]
Stormflow ratio (Q_s/P) (%)	8	1[a]	3	4[b]	3[b]

[a]Model-derived values.
[b]Includes field-based and model-derived data.

streamflow (Q_e/P; the event-water fraction of rainfall; von Freyberg et al., 2018).

3.2.5 | Statistical analyses and determination of response threshold

The Kruskal-Wallis with Tukey's HSD post-hoc test was used to determine whether the median values of the response characteristics differed significantly between the two measurement locations (lower vs. upper weir) and between the two periods (Period 1 *versus* Period 2). Spearman rank correlation (r_s) was used to analyse the relations between event characteristics (rainfall amount and intensity, antecedent wetness) and streamflow response characteristics. Partial linear regression (Jekel & Venter, 2019) was used to determine the presence of any thresholds in these relations. Because streamflow response characteristics are influenced by event size and antecedent conditions, stepwise regression was applied to assess the influence of event characteristics on Q_s, Q_s/P and Q_p. All statistical analyses were performed using Python 3.7, using an arbitrary level of statistical significance of 0.05.

3.3 | Determination of annual streamflow totals

For the period with missing streamflow data (14 May–11 December 2015; 212 days), total streamflow at the lower weir (i.e., the main catchment outlet) was estimated using the HBV model (Lindström et al., 1997; Seibert & Bergström, 2022), a frequently used bucket-type hydrological model. The model was calibrated 50 times using a genetic algorithm by optimizing the non-parametric efficiency (Pool et al., 2018). The ensemble mean streamflow from the calibrated parameter sets was used to estimate the missing streamflow (see Supporting Information section 2.3 for details). These simulations were only used to estimate streamflow for the period with missing data to allow estimation of annual streamflow and stormflow totals for comparison with the data from the 1960s. The modelled data were not used for any other (statistical) analyses. Total rainfall for the period with missing streamflow data was 398 mm (22 rain days with $P \geq 5$ mm).

Annual rainfall, streamflow and stormflow totals were derived for two separate periods: 15 February 2015 until 14 February 2016 and 1 March 2015 until 29 February 2016. The rainfall totals for the two periods differed considerably (1314 and 1103 mm, respectively; Table 1), because February 2015 was very wet (403 mm of rainfall) and February 2016 much drier (126 mm). The available streamflow data did not allow computation of annual totals for the local hydrological year (July–June; Bailly et al., 1974).

4 | RESULTS

4.1 | Total streamflow

Total streamflow (Q) as measured at the catchment outlet was 372 mm during Period 1 (69% of P) and 116 mm (25% of P) for Period 2. The corresponding stormflow totals (Q_s) were 41 mm (8% of P) and 16 mm (3% of P), respectively (Table 1). Total streamflow and stormflow at the upper weir during Period 2 amounted to 100 mm (21% of P) and 27 mm (6% of P), respectively.

Total streamflow for the intermediate period without measured streamflow was estimated at 174 mm (44% of P), yielding an estimated annual streamflow total at the lower weir between 15 February 2015 and 14 February 2016 of 640 mm (±64 mm) or 48 ± 4% of P (Table 1). Total stormflow for the intermediate period was estimated at only 2 mm or 0.5 ± 0.05% of P (Table 1, and Supporting Information section 2.3).

4.2 | Event response characteristics

The descriptive statistics of the rainfall and stormflow events are presented in Tables 2 and 3, respectively. Peak flows occurred earlier at the upper weir compared with the lower weir (Table 3 and Figure 2):

TABLE 2 Summary of the rainfall event characteristics ($n = 50$).

	Lower quartile (Q1)	Median	Upper quartile (Q3)	Maximum
3 day antecedent rainfall (AP_3) (mm)	9	33	53	79
7 day antecedent rainfall (AP_7) (mm)	21	65	121	165
Total amount of rainfall (mm)	7	12	24	71
ASI_{TF2} (mm)	104	115	135	151
ASI_{EUC} (mm)	76	82	86	93
$ASI_{TF2} + P$ (mm)	113	139	152	200
$ASI_{EUC} + P$ (mm)	89	95	106	148
Rainfall event duration (T_p) (min)	200	320	475	1435
Rainfall event centroid (T_{pc}) (min)	55	127	216	864
Maximum 5-min intensity per event (mm h^{-1})	12	223	39	120
Median 5-min intensity per event (mm h^{-1})	2.4	3.6	4.8	9.6
Maximum hourly intensity per event (mm h^{-1})	3.7	6.4	10	33
Median hourly intensity per event (mm h^{-1})	0.7	1.3	3.0	17

Note: ASI is the total amount of water stored in the top 30 cm of the soil at the start of the event.

TABLE 3 Summary of runoff event characteristics, as measured at the catchment outlet (lower weir; $n = 27$) and at the upper weir ($n = 34$).

	Lower quartile (Q1)		Median		Upper quartile (Q3)		Maximum	
	Lower weir	Upper weir	Lower weir	Upper weir	Lower weir	Upper weir	Lower weir	Upper weir
Response lag time (min)	5	5	15	18	65	61	300	215
Stormflow response duration (min)	510	408	625	523	718	645	1680	1920
Lag-to-peak (min)	198	150	255	213	385	301	1120	665
Centroids-lag (min)	190	107	233	141	256	167	344	329
Baseflow (Q_0) (mm h^{-1})	0.04	0.02	0.14	0.04	0.20	0.11	0.27	0.24
Peak flow (Q_p) (mm h^{-1})	0.3	0.1	0.4	0.2	1.1	0.4	3.9	4.6
Stormflow (Q_s) (mm)	0.2	0.2	1.1	0.4	2.6	0.6	9.8	12.7
Stormflow ratio (Q_s/P) (%)	2	3	4	4	9	5	50	22

Note: For 23 and 6 events the streamflow response was insufficient at the lower and upper weir, respectively. These events were not included.

the median lag to peak time at the upper weir was 70 min shorter than that at the lower weir. Soil moisture contents in tree fallow plot TF2 also tended to peak earlier than streamflow at the lower weir, the difference being larger (although not statistically significant) for soil moisture measured at greater depth (Figure 2). For 12 out of 23 events, perched groundwater levels at TF2 also peaked earlier than streamflow. However, perched groundwater levels in the *Eucalyptus* plot, peaked later than the streamflow (by a median value of 327 min for the eight events for which there was a response in both streamflow and groundwater levels; Figure 2).

The stormflow response lag time (i.e., the time between the start of rainfall and the start of stormflow) at the lower weir was marginally correlated with AP_7 ($r_s = 0.29$, $p = 0.05$) and somewhat better with rainfall event duration ($r_s = 0.35$, $p = 0.01$) (Table S4). This was not the case for the stormflow response lag time at the upper weir ($p = 0.8$ and 0.13 for AP_7 and event duration, respectively). Instead, the response lag times at the upper weir were correlated more strongly with the rainfall centroid ($r_s = 0.44$, $p < 0.01$), the response lag time of soil moisture at 15 cm depth ($r_s = 0.72$; plot TF2), and the perched groundwater response lag time at the tree fallow plot TF2 ($r_s = 0.52$, Table S5).

The median stormflow amount (Q_s) was higher for the entire catchment (1.1 mm) than for the upstream sub-catchment (0.4 mm), although the corresponding median stormflow ratios (Q_s/P) were similar (Table 3). Both event total stormflow amount (Q_s) and the stormflow ratio (Q_s/P) at the main outlet were strongly correlated with the antecedent soil moisture plus precipitation index ($ASI_{TF2} + P$) ($r_s = 0.80$ and 0.84, respectively; Figure 3a, Table S4). They were also highly correlated with the maximum perched groundwater level in the tree fallow plot (PWT_{TF2}; $r_s = 0.90$ and 0.82 for Q_s and Q_s/P, respectively) (Figure 4a and Table S4). Total stormflow amount was also correlated with event total rainfall amount ($r_s = 0.78$), event maximum hourly rainfall intensity ($r_s = 0.55$), and event duration ($r_s = 0.51$) (Table S4). Although the event total stormflow amount at the upper

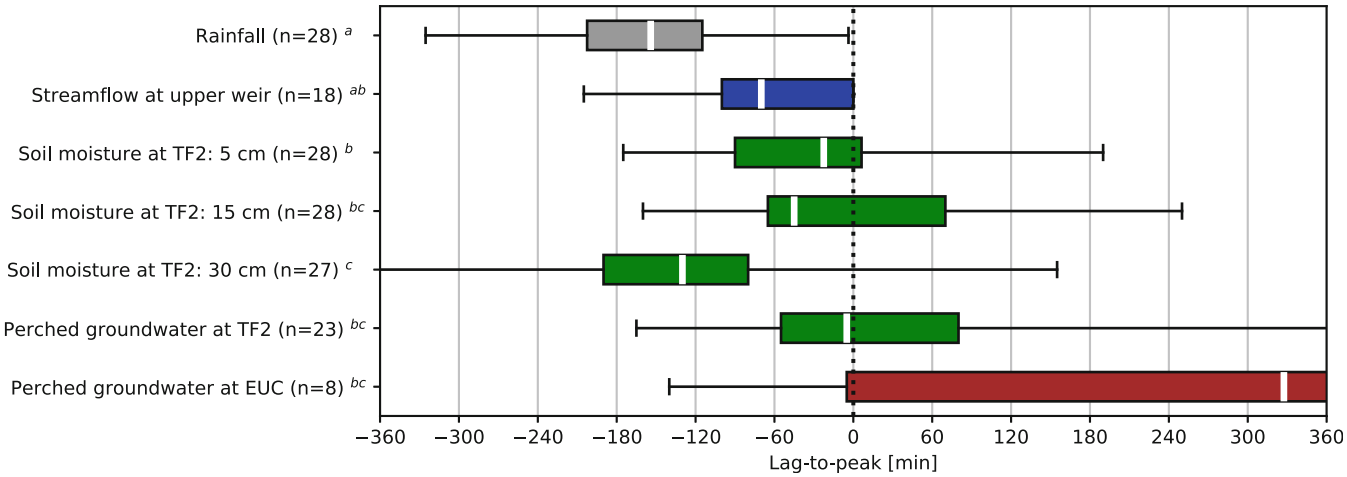

FIGURE 2 Box plots showing the time between peak streamflow at the lower weir ($t = 0$), and the time of the centroid of the rainfall, peak flow at the upper weir, peak soil moisture (SMC) at 5, 15 and 30 cm below the surface in tree fallow plot TF2, and peak perched groundwater levels (PWT) in the tree fallow TF2 and *Eucalyptus* (EUC) plots. Negative values indicate a peak response that is earlier than the peak flow at the lower weir. n = number of events. Note that outliers < −360 min (SMC) and >360 min (PWT) are not shown for visual clarity. Responses that share a similar letter after the name do not have a significantly different median value ($p > 0.05$).

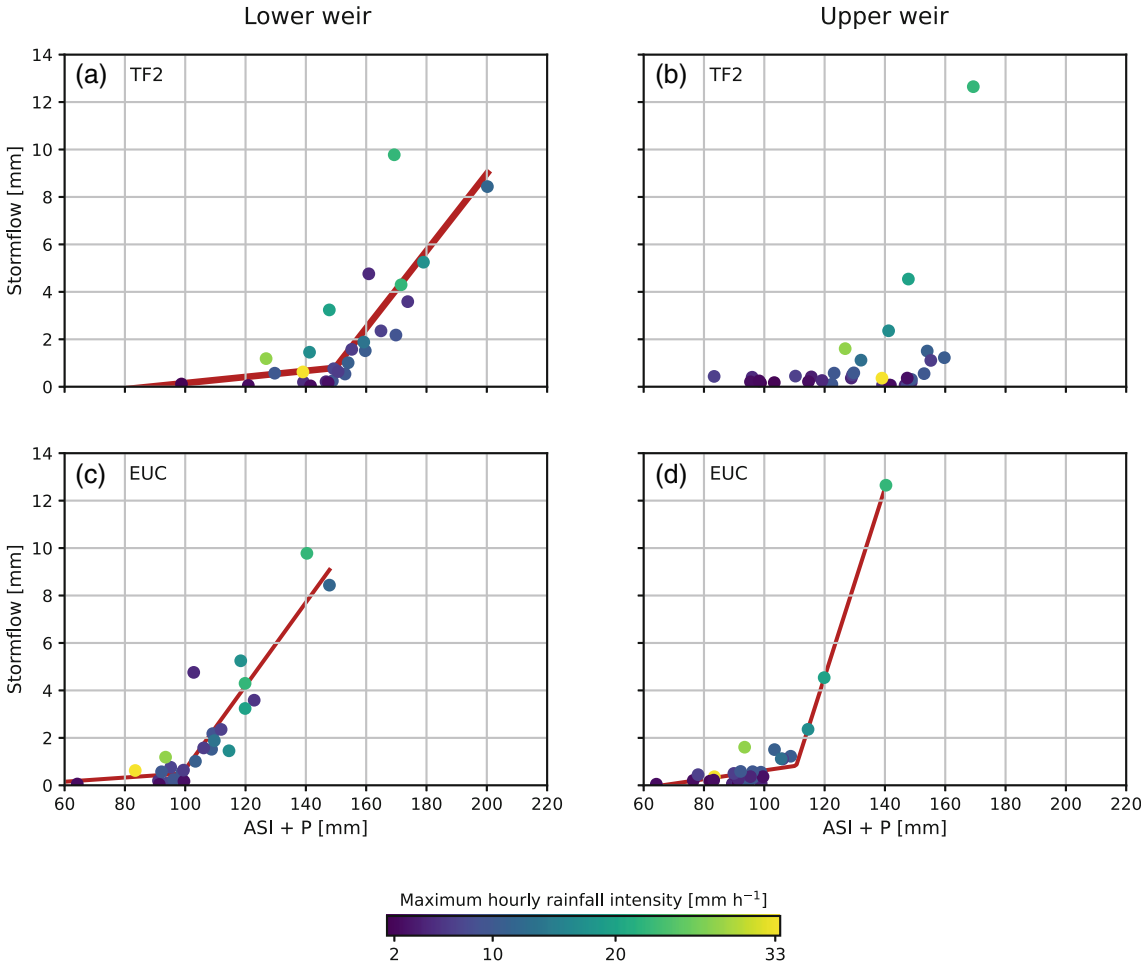

FIGURE 3 Scatterplots of the relation between the total amount of stormflow per event measured at the catchment outlet (a, c) and at the upper weir (b, d) and the antecedent soil moisture plus event rainfall index with soil moisture measured in the tree fallow TF2 ($ASI_{TF2} + P$) (a, b) or the *Eucalyptus* (EUC) plot ($ASI_{EUC} + P$), (c, d). The colour of the symbols reflects the maximum hourly rainfall intensity. The red line shows the best fit based on partial regression analysis. No line means that no significant relation was found.

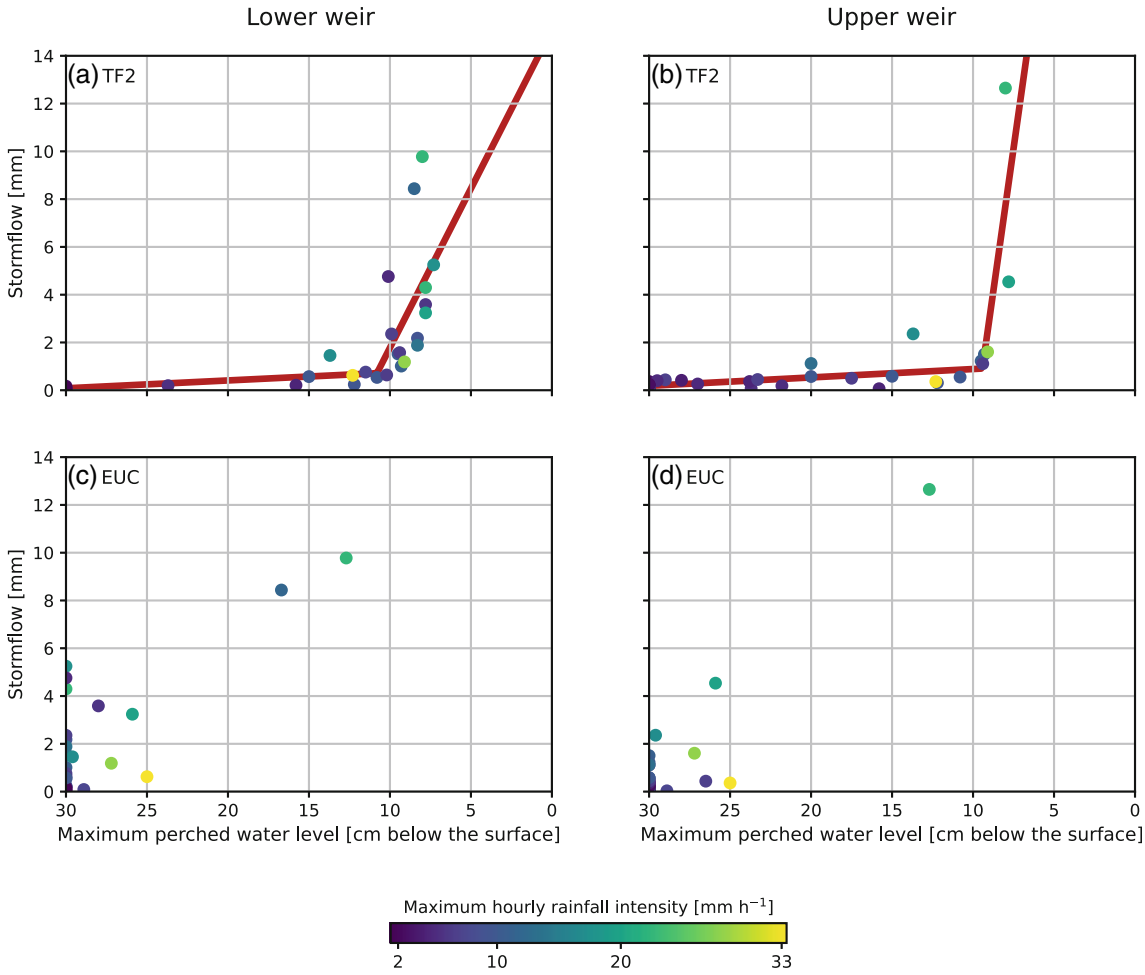

FIGURE 4 Scatterplots of the relation between the amount of stormflow per event measured at the catchment outlet (a, c) and at the upper weir (b, d) and maximum perched groundwater levels measured in the tree fallow TF2 (a, b) or the *Eucalyptus* (EUC) plot (c, d). The colour of the symbols reflects the maximum hourly rainfall intensity. The red line shows the best fit based on partial regression. No line means that no significant relation was found.

weir was also correlated with the maximum perched groundwater level in the tree fallow plot ($r_s = 0.77$), neither the total stormflow amount nor the stormflow ratio were correlated with $ASI_{TF2} + P$ ($r_s = 0.28$, $p = 0.10$ for Q_s; and $r_s = 0.32$, $p = 0.06$ for Q_s/P; Table S5, and Figure 3b). Event total stormflow at the upper weir was correlated most strongly with rainfall amount ($r_s = 0.82$) and, to a lesser extent, the maximum hourly rainfall intensity ($r_s = 0.69$), but not with rainfall event duration ($r_s = 0.25$, $p = 0.16$, Table S5).

Peak flows were generally higher at the lower weir than at the upper weir (upper quartiles of 1.1 and 0.4 mm h^{-1}, respectively) (Table 3). The peak flow rate was highly correlated with the total stormflow amount ($r_s = 0.93$ and 0.77 for the lower and upper weir, respectively; Tables S4 and S5). Not surprisingly, the peak flow rates (Q_p) were also correlated with the antecedent soil moisture plus precipitation index ($r_s = 0.88$ for the lower weir and $r_s = 0.52$ for the upper weir). The peak flow rate was furthermore correlated with the maximum perched groundwater level in the tree fallow plot ($r_s = 0.84$, and $r_s = 0.75$ for the lower and upper weir, respectively), and with the maximum hourly rainfall intensity ($r_s = 0.44$, and $r_s = 0.72$ for the lower and upper weir, respectively).

The stepwise linear regression confirmed the importance of antecedent wetness (either represented by the ASI or pre-storm baseflow Q_0), and event size (P) as dominant predictors of total stormflow amount Q_s. Conversely, rainfall intensity had only a small influence on the stormflow amount and peak flow rate (Tables S4 and S5).

4.3 | Thresholds for stormflow

Clear threshold relationships were identified between the antecedent soil moisture plus precipitation index ($ASI + P$) and event stormflow amount (Q_s) at either weir. Stormflow at the lower weir has an $ASI_{TF2} + P$-*threshold value* of 150 ± 6 mm (standard error) and 99 ± 3 mm for $ASI_{EUC} + P$ (Figure 3a, c). The $ASI_{EUC} + P$-index also showed a clear threshold for stormflow at the upper weir (111 ± 1 mm; Figure 3). This was not the case for the $ASI_{TF2} + P$: the

threshold value for the entire time-series (~140 mm; Figure 3b) was not significant ($p = 0.10$), but those derived separately for the two measurement periods were significant (147 and 137 mm for the first and second period, respectively; Figure 3b, Supporting Information section 5).

There was a similarly clear threshold in the relation between the maximum perched groundwater levels in the tree fallow plot TF2 and total event stormflow at either weir: $PWT_{TF2} = 10.8 \pm 0.1$ cm at the lower weir (Figure 4a) and 9.4 ± 0.2 cm at the upper weir (Figure 4b). Thresholds for perched groundwater levels in the EUC plot were not significant (lower weir: $r_s = 0.08$; upper weir: partial regression, $p = 1.0$; Figure 4c, d, Supporting Information section 5).

4.4 | Event water contributions to streamflow

The four rainfall events for which a two-component hydrograph separation could be applied (Table 4) covered a fairly representative range of events (*cf*. Table 2) in terms of rainfall amount (5–37 mm), maximum 5-min and hourly rainfall intensities (up to 120 and 33 mm h^{-1}, respectively), and antecedent wetness conditions (AP_3: 0.2–53 mm; ASI_{TF2}: 90–144 mm). However, the stormflow ratios for the four events were small (2%–4% at the lower weir, 1%–4% at the upper weir) and the corresponding equivalent minimum contributing areas (MCA) were similar to the fraction of the catchment occupied by the valley-bottom wetlands and paddy fields (3%).

Event-water contributions for these four events ranged from 2% to 16% at the lower weir, and from 6% to 32% at the upper weir (Table 4). The maximum event-water contribution (66 ± 19%) at the lower weir was derived for the largest rainfall event (no. 48, $P = 37$ mm), which also had the highest 5-min rainfall intensity and the driest antecedent condition amongst the four events. The event-water contribution as a percentage of rainfall was low (0.5%) (Table 4). The largest event-water contribution as percentage of rainfall (1%, lower weir) was found for event no. 24 ($P = 34$ mm), which had both the highest ($ASI_{TF2} + P$)-value (139 mm) and the highest maximum hourly rainfall intensity (33 mm h^{-1}; Table 4).

As shown in Figures 5 and 6, the difference in antecedent wetness conditions between events number 24 ('moist') and 48 ('dry') resulted in contrasting responses to rainfall, despite comparable

TABLE 4 Event- and pre-event water contributions at the lower and upper weir for the four examined events.

Event-number		3	24	48	50
Date		17 Feb 2015	1 April 2015	28 Feb 2016	1 March 2016
AP_3 (mm)		33	0	3	53
AP_7 (mm)		92	6	9	55
Rainfall (P) (mm)		5	34	37	16
Rainfall event duration (min)		50	75	225	115
Maximum hourly rainfall intensity (mm h^{-1})		5	33	28	10
Maximum 5-min rainfall intensity (mm h^{-1})		14	84	120	36
$ASI_{TF2} + P$ (mm)		149	139	127	130
Stormflow response duration (min)	Lower weir	[a]	560	535	510
	Upper weir	340	215	575	305
Base flow (Q_0) (mm h^{-1})	Lower weir	0.16	0.15	0.03	0.05
	Upper weir	0.05	0.09	0.02	0.06
Peak flow (Q_p) (mm h^{-1})	Lower weir	[a]	0.3	0.3	0.2
	Upper weir	0.7	0.6	0.7	0.4
Total stormflow (Q_s) (mm)	Lower weir	[a]	0.6	1.2	0.6
	Upper weir	0.2	0.4	1.6	0.6
Stormflow ratio (Q_s/P) (%)	Lower weir	[a]	2	2	4
	Upper weir	3	1	4	4
Average event water contribution (Q_e/Q) (% of streamflow)	Lower weir	2[b]	16	13	7
	Upper weir	6	32		
Uncertainty in pre-event water contribution (%)	Lower weir	11	9	27	42
	Upper weir	10	8		
Maximum event water contribution (% of streamflow)	Lower weir	3[b]	36	66	39
	Upper weir	8	48		
Event water fraction of rainfall (Q_e/P) (% of rainfall)	Lower weir	0.2[b]	1.0	0.5	0.5
	Upper weir	0.5	0.6		

[a]Constant-k method was not applied because the streamflow responses were too small. Empty cells indicate no water samples were available for analysis.
[b]Estimate based on time-series of Q_e and Q_{pe} due to low number of water samples.

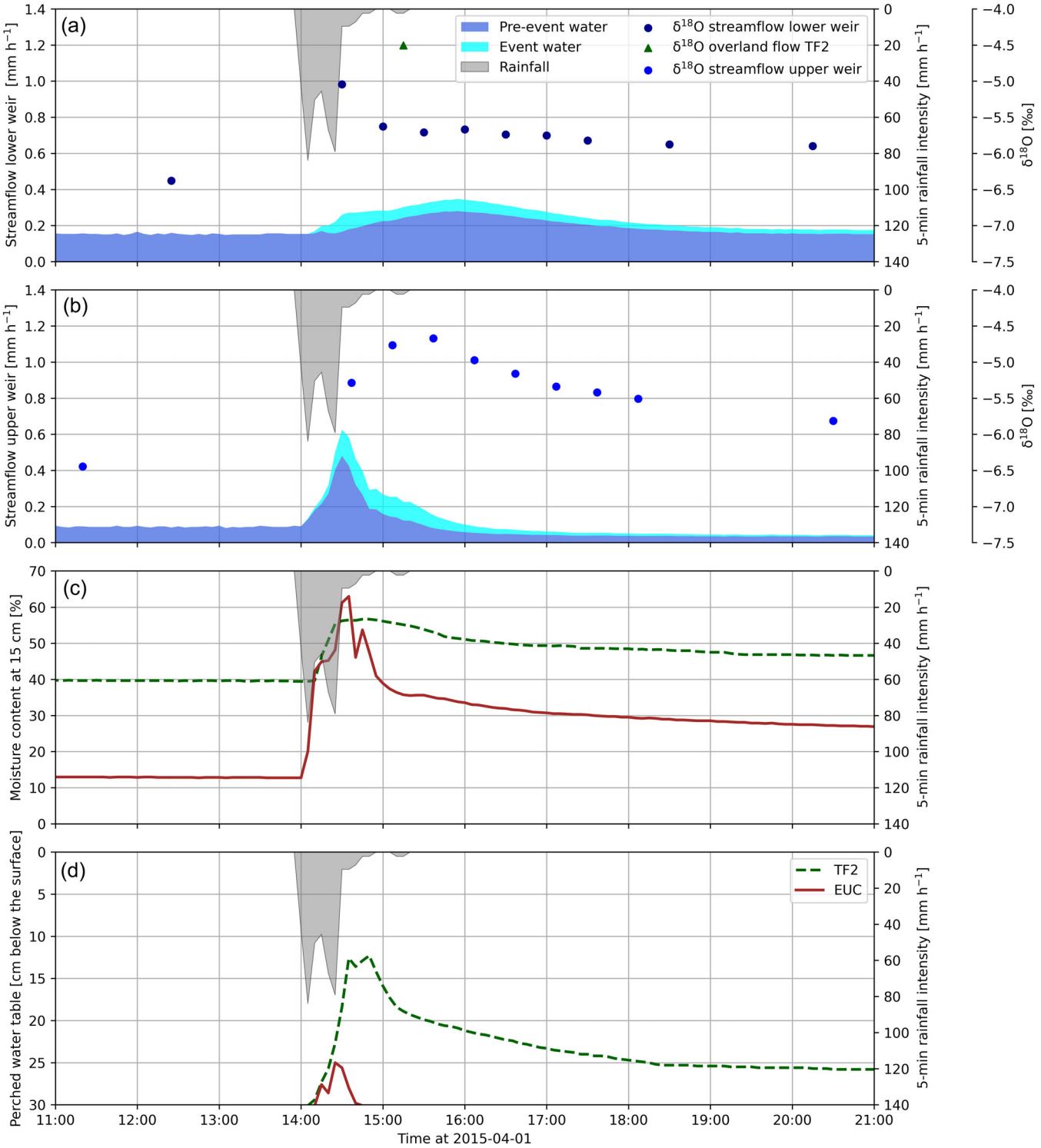

FIGURE 5 Time-series for the 33 mm rainfall event on 1 April 2015 (event no. 24): (a) streamflow, 5-min rainfall intensity, $\delta^{18}O$ in streamflow (circles), and the calculated contributions of pre-event water and event water at the lower weir (outlet) and (b) at the upper weir, (c) volumetric soil moisture contents at 15 cm below the surface in the tree fallow (TF2) and *Eucalyptus* (EUC) plots; and (d) perched groundwater levels in the tree fallow (TF2) and *Eucalyptus* (EUC) plots. The weighted mean $\delta^{18}O$ of the rainfall was −2.67‰.

maximum hourly rainfall intensities (33 and 28 mm h^{-1}, respectively) and total rainfall amounts (33 and 37 mm, respectively). Total storm-flow for event no. 24 was 0.6 mm (MCA: 2%) at the lower weir and 0.4 mm (MCA: 1%) at the upper weir (Figure 5a, b). Peak streamflow was higher at the upper weir (0.6 mm h^{-1}) than at the lower weir (0.3 mm h^{-1}). The event-water contributions during peak streamflow were 23 ± 2% and 19 ± 2%, respectively (Figure 5a, b). About 31 mm (91%) of the rain during this event fell at intensities exceeding the

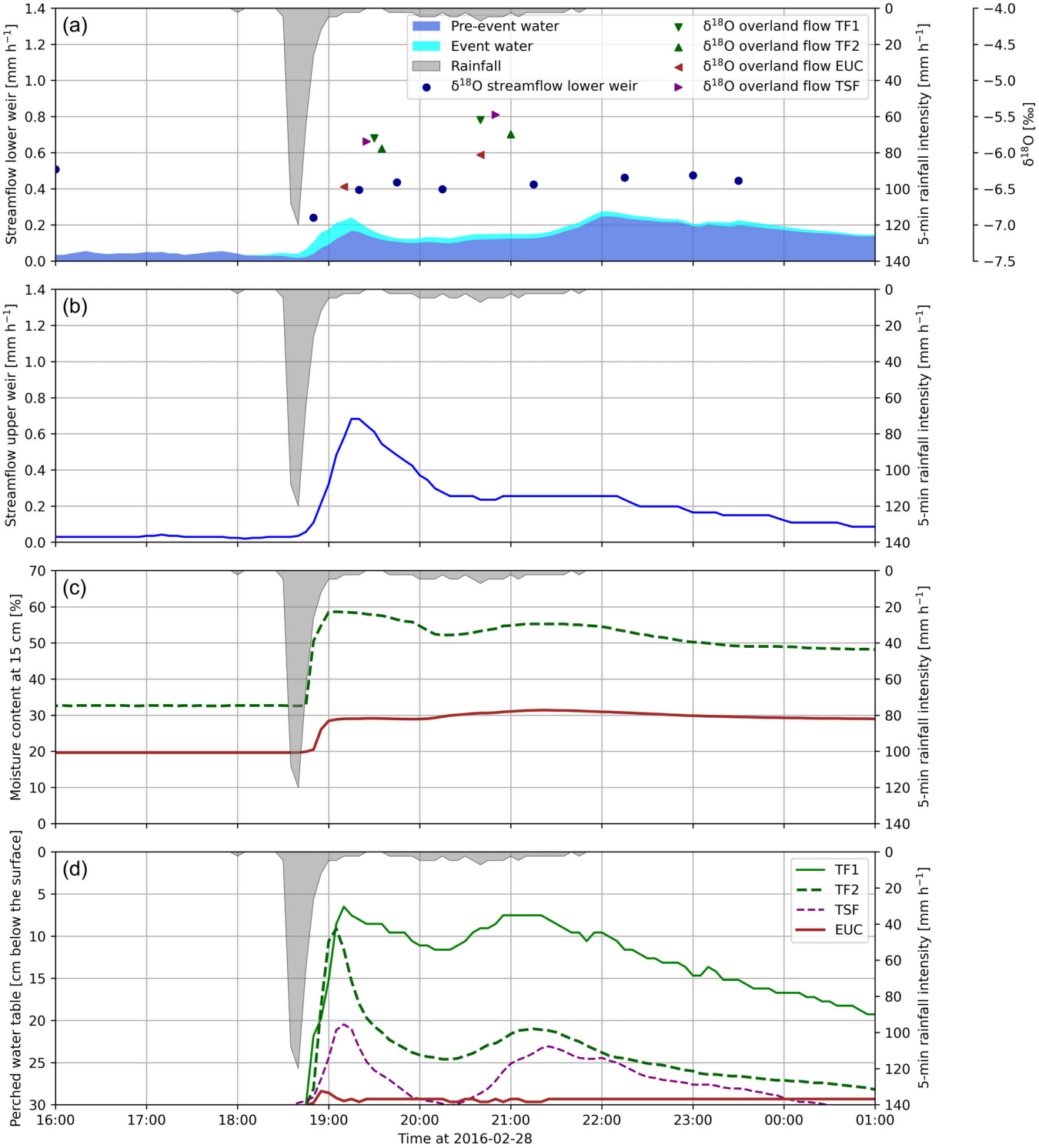

FIGURE 6 Time-series for the 37 mm rainfall event of 28–29 February 2016 (event no. 48): (a) streamflow, 5-min rainfall intensity, $\delta^{18}O$ in streamflow (circles), and the calculated contributions of pre-event water and event water at the lower weir and (b) at the upper weir, (c) volumetric soil water contents at 15 cm below the surface in the tree fallow (TF2) and *Eucalyptus* (EUC) plots; and (d) average perched groundwater levels in the tree fallow plots TF1 and TF2, the terraced shrub fallow (TSF) and the *Eucalyptus* (EUC) plot. The weighted mean $\delta^{18}O$ of the rainfall was −7.45‰.

catchment median K_{sat} at 10–20 cm depth (20 mm h^{-1}), causing the development of a shallow perched water table rising up to ~12 cm below the soil surface (Figure 5d). Some overland flow was observed at the runoff plots: <0.01 mm for the terraced shrub fallow plot, 0.21 mm in tree fallow plot TF2 and 0.25 mm in the EUC plot (no observations were available for tree fallow TF1).

Event no. 48 (Figure 6) lasted longer than event no. 24 (225 min vs. 75 min; Table 4) and included a burst of very high rainfall intensity (maximum 5-min intensity of 120 mm h^{-1}). Peak streamflow in response to this burst was faster and higher at the upper weir (0.7 mm h^{-1}) than at the lower weir (0.2 mm h^{-1}). Event water contributed up 30 ± 8% of streamflow at the lower weir (no data available for the upper weir; Figure 6a, b). Rainfall subsequently continued at a lower intensity (<8 mm h^{-1}), leading to a rapid recession at the upper weir (Figure 6b) and eventually a broad second peak (0.3 mm h^{-1}) at the lower weir (Figure 6a). Event water made up 10 ± 3% of this second peak. Total stormflow was 1.2 mm (MCA: 2%) at the lower weir, and 1.6 mm (MCA: 4%) at the upper weir. Almost three quarters (72%; 27 mm) of the rain fell at intensities above 20 mm h^{-1}, causing top-soil saturation and a perched groundwater table that in some plots almost reached the soil surface (Figure 6d). Overland flow was observed on all four plots, notably in the two tree fallows (≥0.5 mm in TF2 and ≥3.3 mm in TF1; amounts under-estimated because the collectors overflowed; Zwartendijk, van Meerveld, et al., 2020). There was less overland flow at the *Eucalyptus* plot (0.2 mm) and the terraced shrub fallow (0.01 mm). Overland flow from the plots was isotopically more enriched than the streamflow. The difference between the isotopic composition of the flow collected during the high intensity burst of rainfall and the period with lower intensities was largest for the EUC plot (Figure 6a).

5 | DISCUSSION

5.1 | Threshold relationships

Numerous studies in the humid temperate and tropical zones have shown that stormflow volumes and runoff coefficients increase much faster after a certain rainfall event size and/or antecedent wetness threshold is exceeded (Asano & Uchida, 2018; Detty & McGuire, 2010; Litt et al., 2015; Penna et al., 2015; Tobón & Bruijnzeel, 2021; Zhang, Bruijnzeel, et al., 2018). A few studies have shown that stormflow volumes and runoff coefficients increase with event size *and* rainfall intensity (Blume et al., 2007; Norbiato et al., 2009; Zhang, van Meerveld, et al., 2018). Thresholds for increased stormflow occurrence are usually interpreted as the onset of hillslope contributions to streamflow (Detty & McGuire, 2010; McGuire & McDonnell, 2010; Penna et al., 2015). For the Marolaona catchment, stormflow volumes seem to be primarily related to the sum of antecedent moisture in the top 30 cm of the soil and event rainfall (ASI + *P*), and only to a small degree to rainfall intensity (Figure 5a). This suggests that a certain soil water storage capacity needs to be filled before hillslopes contribute measurably to stormflow (*cf*. Penna et al., 2015; Saffarpour et al., 2016; Tobón & Bruijnzeel, 2021).

The $ASI_{TF2} + P$ threshold for increased stormflow at the upper weir at Marolaona was somewhat higher during the first measurement period (February–May 2015; 147 mm) than for the (drier) second period (December 2015–March 2016, 137 mm; Table S8). Since the first period was wetter (Table 1), one would have expected the associated threshold to be lower than that for the drier, second period. This counterintuitive result may be explained by the fact that stormflow amounts at the upper weir were affected by the burning and coppicing of the eucalypt stands in the upper sub-catchment in December 2015 (i.e., during the second period). Eucalypts made up ~38% of the land cover in the upper catchment, with tree fallows roughly covering the remainder (60.5%) (Figure 1). Although the water use of eucalypts under normal conditions would exceed that of the local tree fallows (Ghimire et al., 2018, 2022; Sikka et al., 2003), coppicing caused a temporary drop in soil water uptake (transpiration), leading to temporarily increased soil moisture contents, a correspondingly reduced soil water storage capacity, and hence a lower threshold value for runoff generation. Further, it cannot be excluded that burning the eucalypt fields caused surface soils to become temporarily more hydrophobic (Doerr et al., 2000) and produce infiltration-excess overland flow during times of high rainfall intensity (e.g., in January and February 2016; Zwartendijk, van Meerveld, et al., 2020). Because no major changes occurred in the tree fallows of the upper sub-catchment, the observed dual relationship between stormflow and antecedent wetness in the tree fallows (Figure 3b) must be regarded an artifact of the drastic changes that took place in the eucalypt stands.

Interestingly, the (ASI + *P*)-thresholds associated with increased stormflow at the main catchment outlet are slightly higher than reported by Zwartendijk, van Meerveld, et al. (2020) for overland flow at the plot scale: that is,150 mm vs. 137 mm for $ASI_{TF2} + P$ and 98 vs. 87 mm for $ASI_{EUC} + P$, respectively. Such differences across scales (*cf*. Spence, 2010) may reflect differences in slope gradients and/or interactions with topography (Caviedes-Voullième et al., 2021; Ribolzi et al., 2011), in particular the re-infiltration of overland flow as it moves downslope (Vigiak et al., 2008; Woolhiser et al., 1996). This re-infiltrated water may reach the stream as shallow subsurface stormflow (SSSF) or return flow, depending on slope morphology and changes in soil physical characteristics with depth (Birch et al., 2021a; Birch et al., 2021b; *cf*. McDonnell et al., 2021). Some support for the interpretation that hillslope SSSF rather than return flow/foot-slope SOF may be the dominant runoff contributing process at Marolaona during larger storms may come from the observation that overland flow was estimated to increase by only 0.05 mm and 0.01 mm for every extra mm of ASI + *P* in the TF2 and EUC plot, respectively (Zwartendijk, van Meerveld, et al., 2020). This is roughly an order of magnitude smaller than the corresponding increases in stormflow observed at the main catchment outlet (0.16 and 0.18 mm, for every extra mm of ASI + *P* in the TF2 and EUC plots, respectively; Figure 3a, c). Furthermore, correlations between stormflow amounts (at both weirs) and soil moisture contents and perched water table occurrence were much stronger than those with rainfall intensity (Tables S4 and S5).

5.2 | Runoff generation processes and hillslope-stream connectivity at Marolaona

Stormflow ratios (Q_s/P) and equivalent minimum contributing areas (MCA) were smaller than 3% for most events and roughly matched the percentage of the catchment covered by the stream channel and

adjacent wetlands and rice paddies (Figure 1). Thus, for the ~60% of all events, for which the antecedent moisture storage and rainfall amount were less than the ASI + *P*-threshold, stormflow was likely only generated in the riparian zone (*cf*. Birch et al., 2021a; Bruijnzeel, 1983; Detty & McGuire, 2010; Penna et al., 2015). During wetter conditions or larger events, the storage capacity of the soil above the shallow impeding horizon (Zwartendijk, van Meerveld, et al., 2020) was gradually filled and perched water tables developed (Figure 6), so that the hillslopes became increasingly connected to the stream via rapid lateral subsurface flow and saturated overland flow (Birkel et al., 2021; Bonell & Gilmour, 1978; Saffarpour et al., 2016; Tobón & Bruijnzeel, 2021; Zhang, Bruijnzeel, et al., 2018). Similar findings have been reported for secondary forests in Panamá, where lateral preferential flow within the top 20–30 cm of the soil was the dominant source of storm runoff during large events and (saturation-excess) overland flow only occurred during the largest storms (Birch et al., 2021a, 2021b).

The K_{sat} profiles of the soils at Marolaona (Zwartendijk et al., 2017; Zwartendijk, Ghimire, et al., 2020) imply that for more degraded areas within the catchment (notably those covered by recently abandoned cropped fields under low shrub cover, or fire-related grasslands), saturated overland flow may be a dominant contributor to stormflow. Indeed, van Meerveld et al. (2021) reported annual overland flow fractions of 11% of incident rainfall for a nearby degraded grassland site versus only 2% for a tree fallow and a more mature secondary forest. The median K_{sat} at 20–30 cm depth in the coppiced eucalypt plot (7 mm h^{-1}) was much higher than that in tree fallow TF2 (0.6 mm h^{-1}; Zwartendijk, van Meerveld, et al., 2020), implying a later onset of perched water tables—and therefore a later onset of subsurface flow and overland flow there than at TF2. This contrast is also reflected in the threshold-type relation between stormflow amount and the maximum perched water table level in TF2, whereas no such threshold was identified for the EUC plot (Figure 6). As such, stormflow at the lower weir may be related more closely to the runoff response of tree fallow sites (covering 43% of the catchment) than to sites with eucalypts (30%). This is also shown by the large difference in the lag-to-peak times between the tree fallow and eucalypts plots (Figure 4). Streamflow at the lower weir peaked after soil moisture (Figures 2c, 3c and 4; *cf*. Wilson et al., 1990), whereas the perched water tables at EUC peaked later (and were much less pronounced) than stormflow at the lower weir (Figures 2d and 3d). Perched water tables at EUC also occurred much less frequently than at TF2 ($n = 8$ vs. 23, respectively; Figure 4). All this suggests that subsurface flow from areas with coppiced eucalypts was not an important contributor to peak streamflow in the study area.

Hillslope–stream connectivity at Marolaona required the development of shallow perched water tables on the hillslopes, which were observed as far as 160 m from the stream (<40 m from the divide). The largest stormflow amount measured at the catchment outlet (10 mm, Table 3) was produced during the event of 17 January 2016 ($P = 57$ mm) which occurred after a relatively wet period (ASI + $P_{TF2} = 169$ mm, $AP_7 = 99$ mm). The stormflow ratios for this event, and thus the associated MCAs, were 22% for the upstream sub-catchment and nearly 50% for the entire catchment. Such values imply extensive runoff contributions from the hillslopes in the form of SSSF and SOF, particularly from areas under tree fallow (rather than eucalypts; *cf*. Figures 5 and 6; Zwartendijk, van Meerveld, et al., 2020). Van Meerveld et al. (2019) reported similarly high maximum MCA-values (46%–49%) for a degraded grassland and a reforested catchment on comparatively shallow soils in the Philippines in response to (very) high rainfall. However, overall and maximum event-water contributions were much higher for the grassland catchment (where stormflow was dominated by infiltration-excess overland flow; Cheng et al., 2023), than for the reforested catchment, where stormflow consisted mostly of SSSF and foot-slope SOF (van Meerveld et al., 2019).

The results of the isotope-based hydrograph separations for the four examined rainfall events indicated that stormflow at Marolaona was dominated by pre-event water (Table 4), but event-water contributed substantially during and after peak flows for some of the events (Figures 5 and 6). The four rainfall events were modest in size ($P = 5$–37 mm) and their stormflow ratios and peak flow rates as measured at the lower weir were less than the respective median values for all events (Tables 2–4). The sampled events, therefore, represent situations with a limited degree of hillslope–stream connectivity (*cf*. Ribolzi et al., 2018; Spence, 2010). In other words, event-water contributions might be higher for larger events with greater connectivity between the hillslopes and the stream and larger contributions by rapid SSSF and SOF. However, event-water contributions to stormflow can be relatively high for small events as well, for example, when the stormflow response is mainly caused by rain falling on the stream channel and surrounding saturated areas (Gburek, 1990). During larger storms, event-water contributions tend to be small initially (i.e., once hillslope–stream connectivity is established and SSSF supplies pre-event water), until subsurface flow and (saturated) overland flow gradually contribute more event-water to the stream as the catchment wets up (Birch et al., 2021a, 2021b; Muñoz-Villers & McDonnell, 2013; Penna et al., 2015; Saffarpour et al., 2016; Zhang, Bruijnzeel, et al., 2018).

Streamflow responded faster at the upper weir than at the outlet (Table 2). We attribute this to the small size of the upper sub-catchment and the proximity of a wetland directly upstream of the upper weir (Figure 1). The slower response downstream also highlights the dampening and delay of streamflow as it flows through the channel (Asano & Uchida, 2018; Uchida et al., 2005) and the modulating effects of riparian wetlands and rice paddies (Bullock & Acreman, 2003).

5.3 | Comparison with previous observations in the 1960s

Streamflow in the Marolaona catchment was measured for eight years in the 1960s. Similar measurements were made in a nearby relatively undisturbed rainforest catchment (101 ha) representing baseline conditions (Bailly et al., 1974). Rainfall during our one-year study period (15 February 2015–14 February 2016: 1314 mm; Table 1) was

noticeably lower than during the driest hydrological year (July 1966–June 1967) studied by Bailly et al. (1974) (1517 mm; Figures 7b and S11). Although one would, thus, expect the total water yield in 2015–2016 to be lower than in 1966–1967, the reverse applied: ~48% versus 29% of rainfall, respectively (Figure 7b and S11). In the 1960s, the Marolaona catchment was dominated by dense shrubs and tree fallows, whereas in 2015, coppiced eucalypts covered 30% of the catchment (Figure 1). Before coppicing, the water use of coppiced eucalypts can be expected to be higher (Calder et al., 1993) than for shrubs and young trees (Ghimire et al., 2018; Ghimire et al., 2022) because of the more developed root system of the former (Sikka et al., 2003). Also, prior to the burning of the eucalypts in December 2015, soils under the eucalypts were generally drier and produced less overland flow (Figures 5d and 6d; Zwartendijk, van Meerveld, et al., 2020) and therefore contributed (presumably) less to overall stormflow. As such, one would have expected stormflow ratios to be lower in 2015–2016 than in the 1960s. However, the opposite was found instead (Figure 7).

Although it is not clear how Bailly et al. (1974) exactly determined the end of a storm event (rendering a 1:1 comparison of stormflow ratios somewhat difficult), the stormflow ratio (Q_s/P) was *higher* in 2015–2016 than for the two driest years in the 1960s, that is, 4% in 2015–2016 versus 1% in 1965–1966 and 3% in 1966–1967 (Figures 7c and S11). The higher total water yield and stormflow ratio at Marolaona in 2015–2016 may thus reflect an increase in stormflow production due to progressive land degradation during the additional 40–50 years of slash-and-burn practices (Giertz et al., 2005; Toky & Ramakrishnan, 1981; Zhang, van Meerveld, et al., 2018; Ziegler et al., 2004). Erosion during repeated cropping cycles likely stripped part of the permeable upper soil (*cf.* Zhang et al., 2019); see also the difference in K_{sat}-profiles between degraded grassland and fallow sites in Zwartendijk et al. (2017) and Zwartendijk, Ghimire, et al. (2020). This reduces the soil water storage capacity of the upper soil and results in a more rapid development of perched water tables and associated production of SSSF and SOF (Zwartendijk, van Meerveld, et al., 2020; *cf.* Giertz et al., 2005), thereby increasing the difference

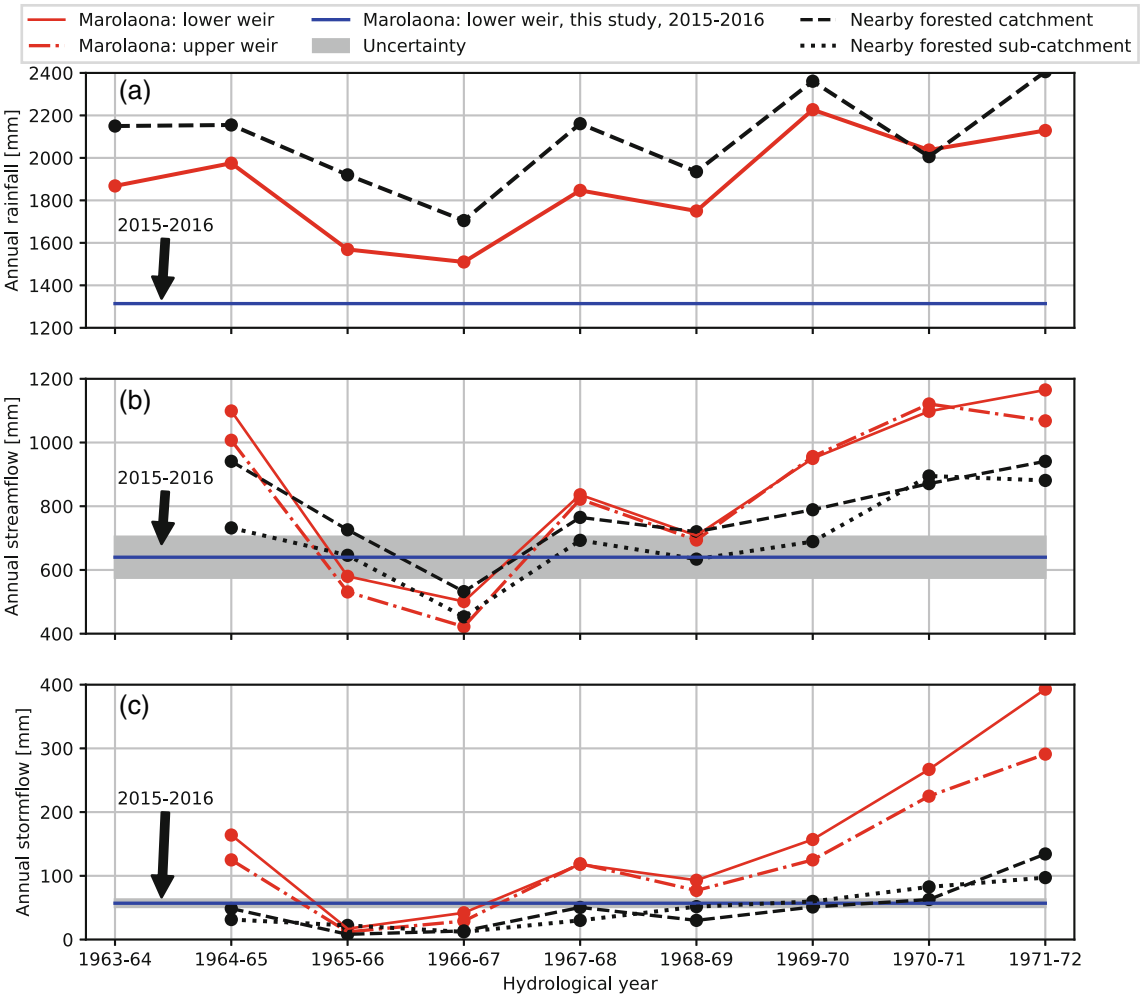

FIGURE 7 Annual rainfall (a), total streamflow (b) and total stormflow (c) for the Marolaona catchment during the 1960s (red lines) and for this study (2015–2016, blue line with an assumed 10% measurement uncertainty for streamflow indicated in grey). For comparison, the data for a nearby forested reference catchment are shown as well (black lines). Data from the 1960s were taken from Annex II in Bailly et al. (1974). Additional information is presented in Supporting Information section 6.

in runoff response with the forested reference catchment (Figures 7c and S11). This can affect local water resources, i.e. increase of downstream flooding and sedimentation (Brookhuis & Hein, 2016; Valentin et al., 2008).

However, due to the seasonality of rainfall at Marolaona these results need to be interpreted with additional caution. Rainfall in the wettest month (February) tends to vary greatly between years (122–449 mm between 1983 and 2013; Metéo Madagascar, 2013). About 280 mm of rainfall were recorded in the second half of February in 2015, but only 55 mm during the same period in 2016. The choice of the starting and ending dates will affect the annual stormflow total (Table 1). Thus, in addition to continued slash-and-burn, one can probably attribute at least part of the observed differences in annual streamflow and stormflow between 2015 and 2016 and the mid-1960s to differences in the timing of rainfall as well (*cf*. Lacombe et al., 2016).

6 | CONCLUSIONS

We examined rainfall-runoff relationships in the 31.7 ha Marolaona catchment in upland eastern Madagascar, where slash-and-burn agriculture has been practiced for more than 70 years. For the majority of the examined events, the stormflow ratio was <3%. Valley-bottom wetlands and rice paddies likely generated most of the stormflow for these events. However, there was a distinct threshold relation between event total stormflow and antecedent moisture storage in the upper 30 cm of the soil plus precipitation (ASI + *P*). Stormflow ratios were much larger for events that exceeded this threshold, reflecting an increase in hillslope–stream connectivity during wetter conditions. Peak flow generally occurred after the onset of perched groundwater tables in the upper 30 cm of the soil on the hillslopes (mostly beneath tree fallows, the dominant land-cover). Stable isotope results for four events that were examined in more detail, indicated that stormflow was dominated by pre-event water (overall event-water contribution ≤16%), but instantaneous event-water contributions were occasionally as high as 66%. Comparison of the streamflow responses at the catchment outlet and at an upstream weir (draining 22% of the total catchment area) suggested that the headwater catchment responded faster due to a direct connection with riparian wetlands. Land cover (notably fallows *versus* coppiced eucalypts) and historic soil erosion influenced the spatial pattern of stormflow generation. Despite the lower rainfall during the study period, annual stormflow and total streamflow (i.e., annual water yield) were higher than recorded for the driest years during the 1960s. This increase in stormflow is most likely due to a reduction in the soil water storage potential caused by the progressive loss of top-soil via erosion during continued slash-and-burn.

AUTHOR CONTRIBUTIONS

B. W. Zwartendijk and C. P. Ghimire collected and compiled the data. B. W. Zwartendijk and H. J. van Meerveld analysed the data. B. W. Zwartendijk and H. J. van Meerveld wrote the first draft. C. P. Ghimire, A. J. Teuling and L. A. Bruijnzeel: validation, review and editing. All co-authors contributed to the final version of the manuscript.

ACKNOWLEDGEMENTS

Fieldwork for this study was conducted within the framework of the P4GES project (Can Paying for Global Ecosystem Services reduce poverty; www.p4ges.org) funded by the ESPA programme of the UK (NE/K010220/1); data were collected with permission of the Madagascar Ministry of Environment, Ecology, Sea and Forests (050/14/MEF/SG/DGF/DCB.SAP/SCB), local authorities and land-owners. Bob Zwartendijk acknowledges financial support from the Dutch Research Council (NWO) (Grant no. 023.016.033). We thank the Marolaona residents for help with the fieldwork, background information, and their overall invaluable contributions to this study, Maafaka Ravelona and Jaona Lahitiana for their indispensable help with the fieldwork and logistics, Nanne Tolsma, Pepijn van Ravesteyn, Razafindrakoto François, Randriamifidimanana Jean Claude, Ihanta Vonifanja, Randriamihary Bernard, Randriamihaja Solofoniaina, and Wendy Zwartendijk for assistance with field measurements and sampling, Maciek Lubczynski and Murat Ucer (University of Twente) for supplying some of the field equipment, Barbara Herbstritt (University of Freiburg, Germany) for the isotope analyses, our colleagues from the Laboratoire des Radio-Isotopes (University of Antananarivo) and Association Mitsinjo for logistical support, and Nick Clarijs for drawing the graphical abstract. We are grateful to two anonymous reviewers for their constructive comments.

DATA AVAILABILITY STATEMENT

Relevant extra information on the field measurements, data analyses, and results are provided in the Supplementary Information. Field data stored at the NERC Environmental Information Data Centre (https://catalogue.ceh.ac.uk/documents/9461f9d7-f7a5-4328-a395-50a3b25da190). Title of the dataset: Hydrometric data and isotope data for streamflow and rainfall in the Marolaona catchment, Madagascar 2015-2016. https://doi.org/10.5285/f93d87ed-7bc4-4d03-9690-3856e6cbbd11.

ORCID

B. W. Zwartendijk https://orcid.org/0000-0002-0581-7330
H. J. van Meerveld https://orcid.org/0000-0002-7547-3270
A. J. Teuling https://orcid.org/0000-0003-4302-2835
C. P. Ghimire https://orcid.org/0000-0002-3715-6311
L. A. Bruijnzeel https://orcid.org/0000-0003-1900-8857

REFERENCES

Andriamananjara, A., Hewson, J., Razakamanarivo, H., Andrisoa, R. A., Ranaivoson, N., Ramboatiana, N., Razafindrakoto, M., Ramifehiarivo, N., Razafimanantsoa, M., Rabeharisoa, L., Ramananantoandro, T., Rasolohery, A., Rabetokotany, N., & Razafimbelo, T. (2016). Land cover impacts on aboveground and soil carbon stocks in Malagasy rainforest. *Agriculture, Ecosystems & Environment*, *233*, 1–15. https://doi.org/10.1016/j.agee.2016.08.030

Asano, Y., & Uchida, T. (2018). The roles of channels and hillslopes in rainfall/run-off lag times during intense storms in a steep catchment.

Hydrological Processes, *32*, 713–728. https://doi.org/10.1002/hyp.11443

Bailly, C., de Coignac, G. B., Malvos, C., Ningre, J. M., & Sarrailh, J. M. (1974). Étude de l'influence du couvert naturel et de ses modifications á Madagascar. Expérimentations en bassins versants élémentaires. In *Cahiers Scientifiques* (Vol. 4, p. 114). Centre Scientifique Forestier Tropical.

Birch, A. L., Stallard, R. F., Bush, S. A., & Barnard, H. R. (2021a). The influence of land cover and storm magnitude on hydrologic flowpath activation and runoff generation in steep tropical catchments of central Panama. *Journal of Hydrology*, *596*, 126138. https://doi.org/10.1016/j.jhydrol.2021.126138

Birch, A. L., Stallard, R. F., Bush, S. A., & Barnard, H. R. (2021b). Precipitation characteristics and land cover control wet season runoff source and rainfall partitioning in three humid tropical catchments in Central Panama. *Water Resources Research*, *57*, e2020WR028058.

Birkel, C., Correa Barahona, A., Duvert, C., Bolanos, S. G., Palma, A. C., Quesada, A. M. D., Murillo, R. S., & Biester, H. (2021). End member and Bayesian mixing models consistently indicate near-surface flowpath dominance in a pristine humid tropical rainforest. *Hydrological Processes*, *35*, e14153. https://doi.org/10.1002/hyp.14153

Blume, T., Zehe, E., & Bronstert, A. (2007). Rainfall-runoff response, event-based runoff coefficients and hydrograph separation. *Hydrological Sciences Journal*, *52*, 843–862. https://doi.org/10.1623/hysj.52.5.843

Bonell, M. (2005). Runoff generation in tropical forests. In M. Bonell & L. A. Bruijnzeel (Eds.), *Forests, Water and People in the Humid tropics* (pp. 314–406). Cambridge University Press. https://doi.org/10.1017/CBO9780511535666.020

Bonell, M., & Gilmour, D. A. (1978). The development of overland flow in a tropical rainforest catchment. *Journal of Hydrology*, *39*, 365–382. https://doi.org/10.1016/0022-1694(78)90012-4

Bonell, M., Purandara, B. K., Venkatesh, B., Krishnaswamy, J., Acharya, H. A. K., Singh, U. V., Jayakumar, R., & Chappell, N. (2010). The impact of forest use and reforestation on soil hydraulic conductivity in the Western Ghats of India: implications for surface and sub-surface hydrology. *Journal of Hydrology*, *391*, 47–62. https://doi.org/10.1016/j.jhydrol.2010/07.004

Bos, M. G. (1989). *Discharge measurement structures* (Third revised ed.). International Institute for Land Reclamation and Improvement/ILRI ISBN 90 70754 150.

Brookhuis, B. J., & Hein, L. G. (2016). The value of the flood control service of tropical forests: A case study for Trinidad. *Forest Policy and Economics*, *62*, 118–124. https://doi.org/10.1016/J.FORPOL.2015.10.002

Bruijnzeel, L. A. (1983). Evaluation of runoff sources in a forested basin in a wet monsoonal environment: a combined hydrological and hydrochemical approach. *International Association of Hydrological Sciences Publication*, *140*, 165–174.

Bullock, A., & Acreman, M. (2003). The role of wetlands in the hydrological cycle. *Hydrology and Earth System Sciences*, *7*, 358–389. https://doi.org/10.5194/hess-7-358-2003

Calder, I. R., Hall, R. L., & Prasanna, K. T. (1993). Hydrological impact of *Eucalyptus* plantation in India. *Journal of Hydrology*, *150*, 635–648. https://doi.org/10.1016/0022-1694(93)90129-W

Caviedes-Voullième, D., Ahmadinia, E., & Hinz, C. (2021). Interactions of microtopography, slope and infiltration cause complex rainfall-runoff behavior at the hillslope scale for single rainfall events. *Water Resources Research*, *57*, e2020WR028127. https://doi.org/10.1029/2020WR028127

Chandler, D. G., & Walter, M. F. (1998). Runoff responses among common land uses in the uplands of Matalom, Leyte, Philippines. *Transactions of the American Society of Agricultural Engineers*, *41*, 1635–1641.

Chazdon, R. (2014). *Second growth: the promise of tropical forest regeneration in an age of deforestation* (p. 472). University of Chicago Press.

Chappell, N. A., Sherlock, M., Bidin, K., Macdonald, R., Najman, Y., & Davies, G. (2007). Runoff Processes in Southeast Asia: Role of Soil, Regolith, and Rock Type. In: Sawada, H., Araki, M., Chappell, N. A., LaFrankie, J. V., Shimizu, A. (Eds.), *Forest Environments in the Mekong River Basin*. Springer. https://doi.org/10.1007/978-4-431-46503-4_1

Cheng, Z., Zhang, J., Yu, B., Chappell, N. A., van Meerveld, H. J., & Bruijnzeel, L. A. (2023). Stormflow response and "effective" hydraulic conductivity of a degraded tropical *Imperata* grassland catchment as evaluated with two infiltration models. *Water Resources Research*, *59*, e2022WR033625. https://doi.org/10.1029/2022WR033625

Curtis, P. G., Slay, C. M., Harris, N. L., Tyukavina, A., & Hansen, M. C. (2018). Classifying drivers of global forest loss. *Science (l York, N.Y.)*, *361*(6407), 1108–1111. https://doi.org/10.1126/science.aau3445

De Moraes, J. M., Schuler, A. E., Dunne, T., Figueiredo, R. D., & Victoria, R. L. (2006). Water storage and runoff processes in plinthic soils under forest and pasture in Eastern Amazonia. *Hydrological Processes*, *20*, 2509–2526. https://doi.org/10.1002/hyp.6213

de Vries, K., Gerold, G., & Bruijnzeel, L. A. (2022). Rainforest conversion to annual cropping and cocoa plantations in montane Sulawesi (Indonesia): impacts on soil hydraulic conductivity and implications for runoff generation. *GEO-ÖKO*, *43*, 175–211.

Detty, J. M., & McGuire, K. J. (2010). Threshold changes in storm runoff generation at a till-mantled headwater catchment. *Water Resources Research*, *46*, W07525. https://doi.org/10.1029/2009WR008102

Dickinson, W. T., & Whiteley, H. (1970). Watershed areas contributing to runoff. *International Association of Scientific Hydrology Bulletin*, *96*, 12–26.

Doerr, S. H., Shakesby, R. A., & Walsh, R. P. D. (2000). Soil water repellency: its causes, characteristics and hydro-geomorphological significance. *Earth-Science Reviews*, *51*, 33–65. https://doi.org/10.1016/S0012-8252(00)00011-8

Elsenbeer, H., Cassel, K., & Castro, J. (1992). Spatial analysis of soil hydraulic conductivity in a tropical rain forest catchment. *Water Resources Research*, *28*(12), 3201–3214. https://doi.org/10.1029/92WR01762

Elsenbeer, H., Newton, B. E., Dunne, T., & de Moraes, J. M. (1999). Soil hydraulic conductivities of latosols under pasture, forest and teak in Rondonia, Brazil. *Hydrological Processes*, *13*, 1417–1422. https://doi.org/10.1002/(SICI)1099-1085(19990630)13:9<1417::AID-HYP816>3.0.CO;2-6

Feng, Y., Ziegler, A. D., Elsen, P. R., Liu, Y., He, X., Spracklen, D. V., Holden, J., Jiang, X., Zheng, C., & Zeng, Z. (2021). Upward expansion and acceleration of forest clearance in the mountains of Southeast Asia. *Nature Sustainability*, *4*, 892–899. https://doi.org/10.1038/s41893-021-00738-y

Fragoso, C., Brown, G. G., Patron, J. C., Blanchart, E., Lavelle, P., Pashanasi, B., Senapati, B., & Kumar, T. (1997). Agricultural intensification, soil biodiversity and agroecosystem function in the tropics: the role of earthworms. *Applied Soil Ecology*, *6*, 17–35.

Fritsch, J. M. (1993). The hydrological effects of clearing tropical rainforest and of implementation of alternative land uses. *International Association of Hydrological Sciences Publication*, *216*, 53–66.

Gafur, A., Jensen, J. R., Borggaard, O. K., & Petersen, L. (2003). Runoff and losses of soil and nutrients from small watersheds under shifting cultivation (*Jhum*) in the Chittagong Hill Tracts of Bangladesh. *Journal of Hydrology*, *274*, 30–46.

Gburek, W. J. (1990). Initial contributing area of a small watershed. *Journal of Hydrology*, *118*, 387–403. https://doi.org/10.1016/0022-1694(90)90270-8

Genereux, D. (1998). Quantifying uncertainty in tracer-based hydrograph separations. *Water Resources Research*, *34*(4), 915–919. https://doi.org/10.1029/98WR00010

Ghimire, C. P., Bruijnzeel, L. A., Bonell, M., Coles, N., Lubczynski, M. W., & Gilmour, D. A. (2014). The effects of sustained forest use on hillslope soil hydraulic conductivity in the Middle Mountains of Central Nepal. *Ecohydrology*, *7*, 478–495. https://doi.org/10.1002/eco.1367

Ghimire, C. P., Bruijnzeel, L. A., Lubczynski, M. W., Zwartendijk, B. W., Odongo, V. O., Ravelona, M., & van Meerveld, H. J. (2018).

Transpiration and stomatal conductance in a young secondary tropical montane forest: contrasts between native trees and invasive understorey shrubs. *Tree Physiology*, *38*, 1053–1070. https://doi.org/10.1093/treephys/tpy004

Ghimire, C. P., van Meerveld, H. J., Zwartendijk, B. W., Bruijnzeel, L. A., Ravelona, M., Lahitiana, J., & Lubczynski, M. W. (2022). Vapour pressure deficit and solar radiation are the major drivers of transpiration in montane tropical secondary forests in eastern Madagascar. *Agricultural and Forest Meteorology*., *326*, 109159.

Giertz, S., Junge, B., & Diekkrüger, B. (2005). Assessing the effects of land use change on soil physical properties and hydrological processes in the sub-humid tropical environment of West Africa. *Physics and Chemistry of the Earth*, *30*(8–10), 485–496. https://doi.org/10.1016/j.pce.2005.07.003

Gomi, T., Sidle, R. C., Ueno, M., Miyata, S., & Kosugi, K. (2008). Characteristics of overland flow generation on steep forested hillslopes of central Japan. *Journal of Hydrology*, *361*, 275–290. https://doi.org/10.1016/j.jhydrol.2008.07.045

Heinimann, A., Mertz, O., Frolking, S., Egelund Christensen, A., Hurni, K., Sedano, F., Parsons Chini, L., Sahajpal, R., Hansen, M., & Hurtt, G. (2017). A global view of shifting cultivation: Recent, current, and future extent. *PLoS One*, *12*(9), e0184479. https://doi.org/10.1371/journal.pone.0184479

Huon, S., de Rouw, A., Bonté, P., Robain, H., Valentin, C., Lefèvre, I., Girardin, C., Le Troquer, Y., Podwojewski, P., & Sengtaheuanghoung, O. (2013). Long-term soil carbon loss and accumulation in a catchment following the conversion of forest to arable land in northern Laos. *Agriculture, Ecosystems and Environment*, *169*, 43–57. https://doi.org/10.1016/j.agee.2013.02.007

Jan, C. D., Chang, C. J., & Lee, M. H. (2006). Discussion of "Design and Calibration of a Compound Sharp-Crested Weir" by J. Martínez, J. Reca, M. T. Morillas, and J. G. López. *Journal of Hydraulic Engineering-ASCE*, *132*(8), 868–871. https://doi.org/10.1061/(ASCE)0733-9429(2006)132:8(868)

Janeau, J. J., Briquet, J. P., Planchon, O., & Valentin, C. (2003). Soil crusting and infiltration on steep slopes in northern Thailand. *European Journal of Soil Science*, *54*, 543–554. https://doi.org/10.1046/j.1365-2389.2003.00494.x

Jekel, F., & Venter, G. (2019). *pwlf: A Python library for fitting 1D continuous piecewise linear functions*. MIT. Homepage:. https://github.com/cjekel/piecewise_linear_fit_py, Contributors:, https://github.com/cjekel/piecewise_linear_fit_py/graphs/contributors

Kennedy, V. C., Zellweger, G. W., & Avanzino, R. J. (1979). Variation of rain chemistry during storms at two sites in northern California. *Water Resources Research*, *15*(3), 687–702. https://doi.org/10.1029/WR015i003p00687

Klaus, J., & McDonnell, J. J. (2013). Hydrograph separation using stable isotopes: Review and evaluation. *Journal of Hydrology*, *505*, 47–64. https://doi.org/10.1016/j.jhydrol.2013.09.006

Lacombe, G., Ribolzi, O., de Rouw, A., Pierret, A., Latsachak, K., Silveira, N., Pham Dinh, R., Orange, D., Janeau, J. L., Soulileuth, B., Robain, H., Taccoen, A., Sengpaathith, P., Mouche, E., Sengtaheuanghoung, O., Tran Duc, T., & Valentin, C. (2016). Contradictory hydrological impacts of afforestation in the humid tropics evidenced by long-term field monitoring and simulation modelling. *Hydrology and Earth System Sciences*, *20*, 2691–2704. https://doi.org/10.5194/hess-20-2691-2016

Lacombe, G., Valentin, C., Sounyafong, P., de Rouw, A., Soulileuth, B., Silvera, N., Pierret, A., Sengtaheuanghoung, O., & Ribolzi, O. (2018). Linking crop structure, throughfall, soil surface conditions, runoff and soil detachment: 10 land uses analyzed in Northern Laos. *Science of the Total Environment*, *616–617*, 1330–1338. https://doi.org/10.1016/j.scitotenv.2017.10.185

Lapides, D. A., David, C., Sytsma, A., Dralle, D., & Thompson, S. (2020). Analytical solutions to runoff on hillslopes with curvature: numerical and laboratory verification. *Hydrological Processes*, *2020*, hyp.13879. https://doi.org/10.1002/hyp.13879

Lavelle, P., Barros, E., Blanchart, E., Brown, G., Desjardins, T., Mariani, L., & Rossi, J. (2001). Soil organic matter management in the tropics: Why feeding the soil macrofauna? *Nutrient Cycling in Agroecosystems*, *61*, 53–61.

Lindström, G., Johansson, B., Persson, M., Gardelin, M., & Bergström, S. (1997). Development and test of the distributed HBV-96 hydrological model. *Journal of Hydrology*, *201*, 272–288. https://doi.org/10.1016/S0022-1694(97)00041-3

Litt, G. F., Gardner, C. B., Ogden, F. L., & Lyons, W. B. (2015). Hydrologic tracers and thresholds: A comparison of geochemical techniques for event-based stream hydrograph separation and flowpath interpretation across multiple land covers in the Panama Canal Watershed. *Applied Geochemistry*, *63*, 507–518. https://doi.org/10.1016/j.apgeochem.2015.04.003

Liu, W. J., Liu, W. Y., Lu, H., Duan, W. P., & Li, H. (2011). Runoff generation in small catchments under a native rain forest and a rubber plantation in Xishuangbanna, southwestern China. *Water and Environment Journal*, *25*, 138–147. https://doi.org/10.1111/j.1747-6593.2009.00211.x

Lozano-Baez, S. E., Cooper, M., Ferraz, S. F. B., Ribeiro Rodrigues, R., Pirastru, M., & Di Prima, S. (2018). Previous land use affects the recovery of soil hydraulic properties after forest restoration. *Water*, *2018* (10), 453. https://doi.org/10.3390/w10040453

Malmer, A., van Noordwijk, M., & Bruijnzeel, L. A. (2005). Effects of shifting cultivation and forest fire. In M. Bonell & L. A. Bruijnzeel (Eds.), *Forests, water and people in the humid tropics* (pp. 533–560). Cambridge University Press.

McDonnell, J. J., Bonell, M., Stewart, M. K., & Pearce, A. J. (1990). Deuterium variations in storm rainfall: Implications for stream hydrograph separation. *Water Resources Research*, *26*(3), 455–458. https://doi.org/10.1029/WR026i003p00455

McDonnell, J. J., Spence, C., Karran, D. J., van Meerveld, H. J., & Harman, C. J. (2021). Fill-and-spill: A process description of runoff generation at the scale of the beholder. *Water Resources Research*, *57*, e2020WR027514. https://doi.org/10.1029/2020WR027514

McGuire, K. J., & McDonnell, J. J. (2010). Hydrological connectivity of hillslopes and streams: Characteristic time scales and nonlinearities. *Water Resources Research*, *46*, W10543. https://doi.org/10.1029/2010wr009341

Météo Madagascar. (2013). Rainfall data CAZ 1983–2013. Technical Report, Météo Madagascar, Ministère des Transports et de la Météorologie, Antananarive, Madagascar.

Moore, R. D. (2004). Introduction to salt dilution gauging for streamflow measurement: Part I. [missing subtitle?]. *Streamline Watershed Management Bulletin*, *7*(4), 20–23.

Moore, R. D. (2005). Introduction to salt dilution gauging for streamflow measurement Part III: Slug injection using salt in solution. *Streamline Watershed Management Bulletin*, *8*(2), 1–6.

Mukul, S. A., & Herbohn, J. (2016). The impacts of shifting cultivation on secondary forests dynamics in the tropics: a synthesis of the key findings and spatio-temporal distribution of research. *Environmental Science & Policy*, *55*, 167–177. https://doi.org/10.1016/j.envsci.2015.10.005

Muñoz-Villers, L. E., & McDonnell, J. J. (2013). Land use change effects on runoff generation in a humid tropical montane cloud forest region. *Hydrology and Earth System Sciences*, *17*, 3543–3560. https://doi.org/10.5194/hess-17-3543-2013

Nespoulous, J., Merino-Martin, L., Monnier, Y., Bouchet, D. C., Ramel, M., Dombey, R., Viennois, G., Mao, Z., Zhang, J. L., Cao, K. F., Le Bissonnais, Y., Sidle, R. C., & Stokes, A. (2019). Tropical forest structure and understorey determine subsurface flow through biopores formed by plant roots. *Catena*, *181*(181), 104061. https://doi.org/10.1016/j.catena.2019.05.007

Norbiato, D., Borga, M., Merz, R., Blöschl, G., & Carton, A. (2009). Controls on event runoff coefficients in the eastern Italian Alps. *Journal of Hydrology*, *375*, 312–325. https://doi.org/10.1016/j.jhydrol.2009.06.044

Patin, J., Mouche, E., Ribolzi, O., Chaplot, V., Sengtahevanghoung, O., Latsachak, K. O., Soulileuth, B., & Valentin, C. (2012). Analysis of runoff production at the plot scale during a long-term survey of a small agricultural catchment in Lao PDR. *Journal of Hydrology*, *426–427*, 79–92. https://doi.org/10.1016/j.jhydrol.2012.01.015

Patin, J., Mouche, E., Ribolzi, O., Sengtahevanghoung, O., Latsachak, K. O., Soulileuth, B., Chaplot, V., & Valentin, C. (2018). Effect of land use on interrill erosion in a montane catchment of Northern Laos: An analysis based on a pluri-annual runoff and soil loss database. *Journal of Hydrology*, *563*, 480–494. https://doi.org/10.1016/j.jhydrol.2018.05.044

Penna, D., van Meerveld, H. J., Oliviero, O., Zuecco, G., Assendelft, R. S., Dalla Fontana, G., & Borga, M. (2015). Seasonal changes in runoff generation in a small forested mountain catchment. *Hydrological Processes*, *29*, 2027–2042. https://doi.org/10.1002/hyp.10347

Podwojewski, P., Orange, D., Jouquet, P., Valentin, C., Van Thiet, N., Janeau, J. L., & Tran, D. T. (2008). Land-use impacts on surface runoff and soil detachment within agricultural sloping lands in Northern Vietnam. *Catena*, *4*, 109–118. https://doi.org/10.1016/j.catena.2008.03.013

Pool, S., Vis, M., & Seibert, J. (2018). Evaluating model performance: towards a non-parametric variant of the Kling-Gupta efficiency. *Hydrological Sciences Journal*, *63*(13–14), 1941–1953. https://doi.org/10.1080/02626667.2018.1552002

Recha, J. W., Lehmann, J., Walter, M. T., Pell, A., Verchot, L., & Johnson, M. (2012). Stream discharge in tropical headwater catchments as a result of forest clearing and soil degradation. *Earth Interactions*, *16–13*, 1–18. https://doi.org/10.1175/2012EI000439.1

Ribolzi, O., Lacombe, G., Pierret, A., Robain, H., Sounyafong, P., de Rouw, A., Soulileuth, B., Mouche, E., Silvera, N., Latxachak, K. O., Sengtaheuanghoung, O., & Valentin, C. (2018). Interacting land use and soil surface dynamics control groundwater outflow in a montane catchment of the lower Mekong basin. *Agriculture, Ecosystems & Environment*, *268*, 90–102. https://doi.org/10.1016/J.AGEE.2018.09.005

Ribolzi, O., Patin, J., Bresson, L. M., Latsachack, K. O., Mouche, E., Sengtaheuanghoung, O., Silvera, N., Thiébaux, J. P., & Valentin, C. (2011). Impact of slope gradient on soil surface features and infiltration on steep slopes in northern Laos. *Geomorphology*, *127*, 53–63. https://doi.org/10.1016/j.geomorph.2010.12.004

Ries, F., Schmidt, S., Sauter, M., & Lange, J. (2017). Controls on runoff generation along a steep climatic gradient in the Eastern Mediterranean. *Journal of Hydrology: Regional Studies*, *9*, 18–33. https://doi.org/10.1016/j.ejrh.2016.11.001

Rijsdijk, A. R., Bruijnzeel, L. A., & Kukuh Sutoto, C. (2007). Runoff and sediment yield from rural roads, trails and settlements in the upper Konto catchment, East Java, Indonesia. *Geomorphology*, *87*, 28–37. https://doi.org/10.1016/j.geomorph.2206.06.040

Robinson, J. S., Sivapalan, M., & Snell, J. D. (1995). On the relative roles of hillslope processes, channel routing, and network geomorphology in the hydrologic response of natural catchments. *Water Resources Research*, *31*, 3089–3101. https://doi.org/10.1029/95WR01948

Saffarpour, S., Western, A. W., Adams, R., & McDonnell, J. J. (2016). Multiple runoff processes and multiple thresholds control agricultural runoff generation. *Hydrology & Earth System Sciences*, *20*, 4525–4545. https://doi.org/10.5194/hess-20-4525-2016

Sandevoir, L., Lespez, L., & Lissak, C. (2023). A connectivity approach to agricultural diffuse pollution in tropical montane catchments dominated by swidden landscapes. *Land*, *2023*(12), 884. https://doi.org/10.3390/land12040784

Scheffler, R., Neill, C., Krusche, A. V., & Elsenbeer, H. (2011). Soil hydraulic response to land-use change associated with the recent soybean expansion at the Amazon agricultural frontier. *Agriculture, Ecosystems and Environment*, *144*(1), 281–289. https://doi.org/10.1016/j.agee.2011.08.016

Seibert, J., & Bergström, S. (2022). A retrospective on hydrological modelling based on half a century with the HBV model. *Hydrology and Earth System Sciences*, *26*, 1371–1388. https://doi.org/10.5194/hess-26-1371-2022

Shougrakpam, S., Sarkar, R., & Dutta, S. (2010). An experimental investigation to characterise soil macroporosity under different land use and land covers of northeast India. *Journal of Earth System Science*, *119*, 655–674. https://doi.org/10.1007/s12040-010-0042-5

Sikka, A. K., Samraj, S., Sharda, V. N., Samraj, P., & Lakshmanan, V. (2003). Low flow and high flow responses to converting natural grassland into bluegum (*Eucalyptus globulus*) in Nilgiris watersheds of South India. *Journal of Hydrology*, *270*, 12–26. https://doi.org/10.1016/S0022-1694(02)00172-5

Sklash, M. G., & Farvolden, R. N. (1979). The role of groundwater in storm runoff. *Journal of Hydrology*, *43*, 45–65. https://doi.org/10.1016/0022-1694(79)90164-1

Spence, C. (2010). A paradigm shift in hydrology: storage thresholds across scales influence catchment runoff generation. *Geography Compass*, *4*, 819–833. https://doi.org/10.1111/j.1749-8198.2010.00341.x

Styger, E., Rakontondramasy, H., Pfeffer, M., Fernandes, E., & Bates, D. (2007). Influence of slash-and-burn farming practices on fallow succession and land degradation in the rainforest region of Madagascar. *Agriculture, Ecosystems & Environment*, *119*, 257–269. https://doi.org/10.1016/j.agee.2006.07.012

Tobón, C., & Bruijnzeel, L. A. (2021). Near-surface water fluxes and their controls in a sloping heterogeneously layered volcanic soil beneath a supra-wet tropical montane cloud forest (NW Costa Rica). *Hydrological Processes*, *35*(11), e14426. https://doi.org/10.1002/hyp.14426

Toky, O., & Ramakrishnan, P. (1981). Run-off and infiltration losses related to shifting agriculture (*Jhum*) in Northeastern India. *Environmental Conservation*, *8*(4), 313–321. https://doi.org/10.1017/S0376892900028125

Toohey, R. C., Boll, J., Brooks, E. S., & Jones, J. R. (2018). Effects of land use on soil properties and hydrological processes at the point, plot, and catchment scale in volcanic soils near Turrialba, Costa Rica. *Geoderma*, *315*, 138–148. https://doi.org/10.1016/j.geoderma.2017.11.044

Uchida, T., & Asano, Y. (2010). Spatial variability in the flowpath of hillslope runoff and streamflow in a meso-scale catchment. *Hydrological Processes*, *24*, 2277–2286. https://doi.org/10.1002/hyp.7767

Uchida, T., Asano, Y., Onda, Y., & Miyata, S. (2005). Are headwaters just the sum of hillslopes? *Hydrological Processes*, *19*, 3251–3261. https://doi.org/10.1002/hyp.6004

Valentin, C., Agus, F., Alamban, R., Boosaner, A., Bricquet, J. P., Chaplot, V., de Guzman, T., de Rouw, A., Janeau, J. L., Orange, D., Phachomphonh, K., Phai, D. D., Podwojewski, P., Ribolzi, O., Silvera, N., Subagyono, K., Thiébaux, J. P., Toan, T. D., & Vadari, T. (2008). Runoff and sediment losses from 27 upland catchments in Southeast Asia: impacts of rapid land use changes and conservation practices. *Agriculture, Ecosystems & Environment*, *128*, 225–238. https://doi.org/10.1016/j.agee.2008.06.004

van Meerveld, H. J., Jones, J. P. G., Ghimire, C. P., Zwartendijk, B. W., Lahitiana, J., Ravelona, M., & Mulligan, M. (2021). Forest regeneration can positively contribute to local hydrological ecosystem services: Implications for forest landscape restoration. *Journal of Applied Ecology*, *58*, 755–765. https://doi.org/10.1111/1365-2664.13836

van Meerveld, H. J., Zhang, J., Tripoli, R., & Bruijnzeel, L. A. (2019). Effects of reforestation of a degraded *Imperata* grassland on dominant flow pathways and streamflow responses in Leyte, the Philippines. *Water Resources Research*, *55*, 4128–4148. https://doi.org/10.1029/2018WR023896

Van Vliet, N., Mertz, O., Heinimann, A., Langanke, T., Pascual, U., Schmook, B., Adams, C., Schmidt-Vogt, D., Messerli, P., Leisz, S.,

Castella, J. C., Jorgensen, L., Birch-Thomsen, T., Hett, C., Bech-Bruun, T., Ickowitz, A., Vu, K. C., Yasuyuki, K., Fox, J., … Ziegler, A. D. (2012). Trends, drivers and impacts of changes in swidden cultivation in tropical forest-agriculture frontiers: A global assessment. *Global Environmental Change*, *22*(2), 418–429. https://doi.org/10.1016/j.gloenvcha.2011.10.009

Vigiak, O., Ribolzi, O., Pierret, A., Sengtaheuanghoung, O., & Valentin, C. (2008). Trapping efficiencies of cultivated and natural riparian vegetation of Northern Laos. *Journal of Environmental Quality*, *37*, 889–897. https://doi.org/10.2134/jeq2007.0251

von Freyberg, J., Studer, B., Rinderer, M., & Kirchner, J. W. (2018). Studying catchment storm response using event and pre-event water volumes as fractions of rainfall rather than discharge. *Hydrology and Earth System Sciences*, *2018*, 5847–5865. https://doi.org/10.5194/hess-22-5847-2018

Western, A. W., Grayson, R. B., Blöschl, G., Willgoose, G. R., & McMahon, T. A. (1999). Observed spatial organization of soil moisture and its relation to terrain indices. *Water Resources Research*, *35*(3), 797–810. https://doi.org/10.1029/1998WR900065

Wilson, G. V., Jardine, P. M., Luxmoore, R. J., & Jones, J. R. (1990). Hydrology of a forested hillslope during storm events. *Geoderma*, *46*, 119–138. https://doi.org/10.1016/0016-7061(90)90011-W

Woolhiser, D. A., Smith, R. E., & Giraldez, J.-V. (1996). Effects of spatial variability of saturated hydraulic conductivity on Hortonian overland flow. *Water Resources Research*, *32*(3), 671–678. https://doi.org/10.1029/95WR03108

Xu, C., Yang, Z., Qian, W., Chen, S., Liu, X., Lin, W., Xiong, D., Jiang, M., Chang, C. T., Huang, C., Jr., & Yang, Y. (2019). Runoff and soil erosion responses to rainfall and vegetation cover under various afforestation management regimes in subtropical montane forest. *Land Degradation and Development*, *30*, 1711–1724. https://doi.org/10.1002/ldr.3377

Zhang, J., Bruijnzeel, L. A., Quiñones, M. C., Tripoli, R., Asio, V. B., & van Meerveld, H. J. (2019). Soil physical characteristics of a degraded tropical grassland and a 'reforest': implications for runoff generation. *Geoderma*, *333*, 163–177. https://doi.org/10.1016/j.geoderma.2018.07.022

Zhang, J., Bruijnzeel, L. A., Tripoli, R., & van Meerveld, H. J. (2018). Water budget and run-off response of a tropical multispecies "reforest" and effects of typhoon disturbance. *Ecohydrology*, *12*, e2055. https://doi.org/10.1002/eco.2055

Zhang, J., van Meerveld, H. J., Tripoli, R., & Bruijnzeel, L. A. (2018). Runoff response and sediment yield of a landslide-affected fire-climax grassland micro-catchment (Leyte, the Philippines) before and after passage of typhoon Haiyan. *Journal of Hydrology*, *65*, 524–537. https://doi.org/10.1016/j.jhydrol.2018.08.016

Ziegler, A., Giambelluca, T., Tran, L., Vana, T., Nullet, M., Fox, J., Vien, T., Pinthong, J., Maxwell, J., & Evett, S. (2004). Hydrological consequences of landscape fragmentation in mountainous northern Vietnam: Evidence of accelerated overland flow generation. *Journal of Hydrology*, *287*, 124–146. https://doi.org/10.1016/j.jhydrol.2003.09.027

Ziegler, A. D., Bruun, T. B., Guardiola-Claramonte, M., Giambelluca, T. W., Lawrence, D., & Thanh Lam, N. (2009). Environmental consequences of the demise in swidden cultivation in montane mainland Southeast Asia: Hydrology and geomorphology. *Human Ecology*, *37*, 361–373.

Zimmermann, B., Elsenbeer, H., & de Moraes, J. (2006). The influence of land-use changes on soil hydraulic properties: implications for runoff generation. *Forest Ecology and Management*, *222*, 29–38. https://doi.org/10.1016/j.foreco.2005.10.070

Zwartendijk, B. W., Ghimire, C. P., Ravelona, M., Lahitiana, J., & van Meerveld, H. J. (2020). Soil hydrological characteristics for three areas in the Corridor Ankeniheny-Zahamena (CAZ), Madagascar. NERC Environmental Information Data Centre. https://doi.org/10.5285/7987c6d4-973d-436d-a13b-c52997d0bce5

Zwartendijk, B. W., van Meerveld, H. J., Ghimire, C. P., Bruijnzeel, L. A., Ravelona, M., & Jones, J. P. G. (2017). Rebuilding soil hydrological functioning after swidden agriculture in eastern Madagascar. *Agriculture, Ecosystems & Environment*, *239*, 101–111. https://doi.org/10.1016/j.agee.2017.01.002

Zwartendijk, B. W., van Meerveld, H. J., Ghimire, C. P., Ravelona, M., Lahitiana, J., & Bruijnzeel, L. A. (2020). Soil water- and overland flow dynamics in a tropical catchment subject to long-term slash-and-burn agriculture. *Journal of Hydrology*, *582*, 124287. https://doi.org/10.1016/j.jhydrol.2019.124287

SUPPORTING INFORMATION

Additional supporting information can be found online in the Supporting Information section at the end of this article.

How to cite this article: Zwartendijk, B. W., van Meerveld, H. J., Teuling, A. J., Ghimire, C. P., & Bruijnzeel, L. A. (2023). Rainfall-runoff responses and hillslope moisture thresholds for an upland tropical catchment in Eastern Madagascar subject to long-term slash-and-burn practices. *Hydrological Processes*, *37*(8), e14937. https://doi.org/10.1002/hyp.14937